Physics Reports 531 (2013) 173–199

Contents lists available at ScienceDirect

Physics Reports

journal homepage: www.elsevier.com/locate/physrep

Oscillation quenching mechanisms: Amplitude vs. oscillation death

Aneta Koseska [a,b,*], Evgeny Volkov [c], Jürgen Kurths [a,d]

[a] Institute of Physics, Humboldt University Berlin, D-10099 Berlin, Germany
[b] Department of Systemic Cell Biology, Max Planck Institute for Molecular Physiology, Otto-Hahn-Str. 11, 44227, Dortmund, Germany
[c] Department of Theoretical Physics, Lebedev Physical Inst., Leninskii 53, Moscow, Russia
[d] Potsdam Institute for Climate Impact Research, D-14412 Potsdam, Germany

ARTICLE INFO

Article history:
Accepted 20 June 2013
Available online 3 July 2013
editor: I. Procaccia

Keywords:
Coupled oscillators
Oscillation death
Amplitude death

ABSTRACT

Oscillation quenching constitutes a fundamental emergent phenomenon in systems of coupled nonlinear oscillators. Its importance for various natural and man-made systems, ranging from climate, lasers, chemistry and a wide range of biological oscillators can be projected from two main aspects: (i) suppression of oscillations as a regulator of certain pathological cases and (ii) a general control mechanism for technical systems. We distinguish two structurally distinct oscillation quenching types: *oscillation* (*OD*) and *amplitude death* (*AD*) phenomena. In this review we aim to set clear boundaries between these two very different oscillation quenching manifestations and demonstrate the importance for their correct identification from the aspect of theory as well as of applications. Moreover, we pay special attention to the physiological interpretation of *OD* and *AD* in a large class of biological systems, further underlying their different properties. Several open issues and challenges that await further resolving are also highlighted.

Contents

1. Introduction 174
2. General description of oscillation quenching: amplitude *vs.* oscillation death 176
   2.1. Oscillation death phenomenon 176
   2.2. Amplitude death 177
   2.3. Turing bifurcation characterizes the transition from AD to OD 177
3. Oscillation death: generation principle, characteristics and applications 178
   3.1. Biological oscillators 178
      3.1.1. Oscillators with an *N*-shaped nullcline: genetic, calcium and membrane relaxation oscillators 178
      3.1.2. Emergence of *OD* in system of coupled repressilators 183
   3.2. Chemical oscillators 184
      3.2.1. Oscillators with model-specific phase portraits 184
   3.3. Chaotic oscillators 185
   3.4. Neuronal oscillators 186
4. Oscillation death dominance: role of parameter mismatches 187

* Corresponding author at: Department of Systemic Cell Biology, Max Planck Institute of Molecular Physiology, Otto-Hahn-Str. 11, 44227 Dortmund, Germany Tel.: +49 0 231 133 2252.
E-mail address: Aneta.Koseska@mpi-dortmund.mpg.de (A. Koseska).

0370-1573/$ – see front matter © 2013 Elsevier B.V. All rights reserved.
http://dx.doi.org/10.1016/j.physrep.2013.06.001

5. OD-related regimes 187
5.1. Inhomogeneous limit cycles 188
5.2. Mixed-mode oscillations 188
5.3. Partial OD 189
6. Characteristics of the AD phenomenon 190
6.1. *AD* via eigenfrequency distribution of the coupled oscillators 190
6.2. Time-delayed interactions and occurrence of *AD* 190
6.3. Transition between *AD* and *OD* in neuronal systems and physiological implications 192
6.4. Partial amplitude death 193
7. Summary 193
Acknowledgments 194
Appendix A. Mathematical models 194
References 196

List of Abbreviations and Symbols

AD	Amplitude death
OD	Oscillation death
ODD	Oscillation death dominance
IHSS	Inhomogeneous steady state
IHLC	Inhomogeneous limit cycle
HB	Hopf bifurcation
PB	Pitchfork bifurcation
BZ	Belousov–Zhabotinsky reaction
AI	Autoinducer molecule
ε	Stiffness parameter
d	Coupling coefficient
Δ	Frequency mismatch
τ	Time delay

1. Introduction

Coupled oscillators constitute an effective and popular paradigm for the study of interacting oscillatory processes in physics, chemistry, biology, neuroscience, climate research and engineering. Examples include arrays of Josephson junctions [1,2], semiconductor lasers [3,4], relativistic magnetrons [5], chemical reactions [6–9], circadian pacemakers [10,11], neurons [12,13], power grids [14] and a variety of other biological processes [15,16]. This research is even more strengthened due to the fact that natural systems, which we tend to understand and exploit, are rarely isolated, and the interactions between them are frequently inevitable, determining the system's properties. Thus, the analysis of various oscillatory systems has provided striking examples of different types of dynamical behavior that can be induced by the presence of coupling. In general, the dynamical behavior observed in the different cases depends both on the coupling organization and strength, as well as on the characteristics of the individual oscillators composing the systems.

To start with, weak coupling of nonlinear oscillators leads to *synchronization*, a fundamental nonlinear phenomenon in various fields of science [17–19]. Despite various physical applications [20], it has been shown that synchronization is inevitable for proper functioning of various biological systems. In mammals, for example, a coherent circadian output is a result of synchronization of thousands of diverse neurons in the suprachiasmatic nucleus [21–24]. Moreover, it has been also shown that synchronization is crucial for the formation of somites in the course of vertebrate segmentation [25]. However, there is also evidence that synchronization plays a key role in the pathogenesis of several neurological diseases, such as Parkinson's disease and essential tremor, i.e. [26–29] and references therein. For example, it is hypothesized that Parkinsonian symptoms result from a synchronized pacemaker-like activity of a population of many thousands of neurons in the basal ganglia [30,31].

Another fundamental emergent phenomenon in coupled system is *oscillation quenching*. The importance of this phenomenon can be projected from the following perspectives: (i) oscillation suppression or disruption of oscillations is significantly relevant in pathological cases of neuronal disorders such as Alzheimer's and Parkinson's disease; and (ii) it can serve as a control mechanism and an efficient regulator of system's dynamics (i.e. it can lead to stabilization in case of coupled lasers [32,33]). Thus, this behavior is characteristic and has been observed for a wide range of natural and man-made systems, ranging from climate systems [34], lasers [35,32,33], electronic circuits [36,37], systems exhibiting chaotic dynamics [38,39], chemical systems [8,40], neurons [41,42], biological networks [43–45], etc.

In general, we distinguish between two different types of oscillation quenching phenomena which differ both in the background generation mechanisms, as well as in their manifestation: *oscillation* and *amplitude death*. Next, we give a general introduction to these phenomena.

Let us define a system of N coupled m-dimensional oscillators, each characterized with a stable limit cycle:

$$\frac{dx_i^j}{dt} = F(x_i^j, k) + d_i^j \sum_{j=1}^{N} (x_i^j - x_i^{j-1}) \tag{1}$$

where $i = 1, \ldots, m$ and $j = 1 \cdots N$, x_i is the phase variable, F is a nonlinear function, and d_i^j denotes a local coupling mechanism (i.e. scalar or vector coupling). Generally, Eq. (1) can be easily modified to incorporate other coupling types, i.e. direct or global coupling.

In the phase space, the system generates an N-dimensional torus T^N in the product space $R^{m\times N} = R^m \times \cdot \times R^m$, by taking the Cartesian product of the limit cycles for the individual oscillators. If the oscillators are identical, the torus is covered by an n-parameter family of periodic solutions. However, only a number of them will persist when coupling is present, depending both on the nature and the strength of the coupling.

For N coupled oscillators, on the other hand, linear coupling d_i^j can also produce a number of different steady states, some of them are stable and have their own basins of attraction. In this case, the phase space is "split" between the limit cycles and the steady states which coexist. Moreover, in the case of N interacting limit cycles, under well-defined conditions, the so-called *inhomogeneous steady state* (*IHSS*) can appear. This phenomenon is characterized with different values of the phase variables x_i^j in the phase space, which depend on the index of the oscillator, j. We will refer to this phenomenon as the *oscillation death* (*OD*) phenomenon.

The idea of *IHSS* was already originated by Turing in his seminal paper *"The chemical basis of morphogenesis"* [46], where he described the principles of symmetry-breaking of a stable steady state, which can then give raise to stable patterns. Several years later, Prigogine and Lefever used the non-equilibrium thermodynamic formalism and extended this phenomenon on diffusion-coupled oscillating regimes by showing that: there exists a symmetry-breaking instability beyond which the stable steady state solution corresponds to an inhomogeneous situation (a transition from a homogeneous to an inhomogeneous steady state), maintained through a subtle balance between reaction rates and diffusion [47]. Several experimental realizations followed in the upcoming years [8,40] etc.

On the other hand, when increasing the coupling in the system of N coupled limit cycle oscillators (d_i^j in Eq. (1)), the dissipation in the system rises to an extent such that the phase space collapses: the oscillators pull each other off the limit cycles and collapse into a fix point. This fix point can be that of the origin, or an entirely new one, created by the coupling. This means that in contrast to the previous case, where oscillation death or *IHSS* is observed, the phase space is not shared here—either a limit cycle or a fix point exists. Thus, the suppression of oscillations manifested through the existence of a *homogeneous steady state* (*HSS*) [48,49,41,50,51] we will denote further as *amplitude death* (*AD*). We note here that in the literature, the terminology "phase death" can be also found. However, this phenomenon can be always classified in one of the two oscillation quenching types we already defined [52,53].

Although mathematically, the background mechanisms, as well as the manifestation of oscillation and amplitude death phenomena can be clearly distinguished, misinterpretation of these two oscillation quenching types can be found often in the literature. However, due to their significantly different representation, as an inhomogeneous (*OD*) vs. homogeneous (*AD*) steady state, we believe that it is necessary to establish a clear distinction in their properties as well as the terminology used. Moreover, from the viewpoint of dynamical control, both oscillation quenching types allow the generation of two *completely different* dynamical regimes with different influence and meaning: i.e. *OD* constitutes a well-known phenomenon in neurons, the "winner-take-all" situation [54,42], whereas *AD* mainly serves to suppress neuronal oscillations [49]. Moreover, it has been shown that the *IHSS* (*OD*) can be related as a background mechanism of cellular differentiation [55,56], whereas *AD* is mainly used as a stabilization control in physical or chemical systems [32,33].

This report therefore aims at setting clear boundaries between oscillation and amplitude death phenomena, characterizing their background mechanisms of occurrence, manifestation properties, as well as applications in various fields, ranging from biological, chemical, chaotic and neuronal oscillators, etc. Moreover, we overview as well dynamical regimes which are, in most of the cases, directly related to oscillation quenching phenomena, such as *oscillation death dominance* (*ODD*) [57,58], inhomogeneous limit cycles [59,55], partial amplitude death [60], etc. Our intention is that this review serves as a guideline to distinguish the main characteristics of oscillation quenching regimes, improving and broadening its applicability in various areas.

The paper is organized as follows. In Section 2 we give a general description of both oscillation quenching types, *AD* and *OD*, for a paradigmatic model of coupled Landau–Stuart oscillators, and stress their difference by characterizing the transition scenario between *AD* and *OD*, as discussed in [61]. In Section 3 we focus on the *OD* phenomenon, and overview its generation principle and characteristics. Various models, ranging from biological, and chemical to chaotic systems are discussed in this context. Next, an analysis how *OD* can dominate the parameter space is presented in Section 4. Moreover, in Section 5 we discuss also oscillatory dynamical solutions which are in most of the cases related to the *OD* regime, such as inhomogeneous limit cycles, mixed-mode oscillations and partial *OD*. The main routes to *AD* and its related dynamical solutions, as well as the different interpretation of both oscillation quenching regimes for natural systems are given in Section 6. Finally, a brief summary and outlook are presented in Section 7.

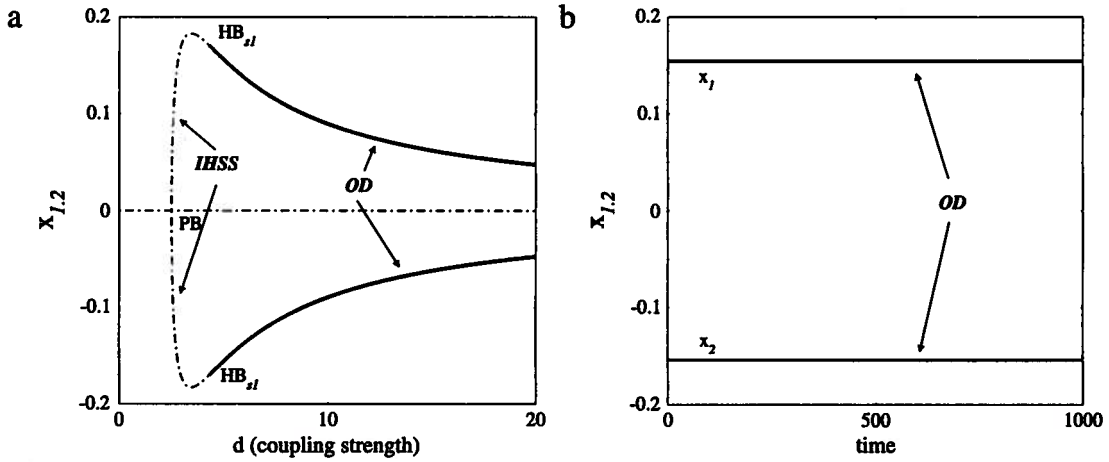

Fig. 1. Manifestation of oscillation death (stable inhomogeneous steady state) for $N = 2$ coupled Landau–Stuart oscillators. (a) Bifurcation diagram obtained by variation of d, to illustrate *OD* for identical frequencies ($\omega_1 = \omega_2 = 2$). Dashed-dotted lines denote unstable steady states and thick solid lines denote stable *OD*. (b) Time-series representation of *OD* for $d = 5.1$.

2. General description of oscillation quenching: amplitude *vs.* oscillation death

As already noted, oscillation quenching mechanisms can be classified in two different types, depending on their manifestation properties: *oscillation death*, characterized with a presence of an *inhomogeneous steady state*, and *amplitude death*, resulting in the formation of a *homogeneous steady state*. To clarify their differences, we use here the paradigmatic model of a Landau–Stuart oscillator, described with the equation of motion:

$$\frac{dz}{dt} = (1 + i\omega - |z|^2)z. \tag{2}$$

Here, ω is the eigenfrequency of the oscillator, and $z(t) = x(t) + iy(t)$ is the phase variable.

2.1. Oscillation death phenomenon

Coupling two Landau–Stuart oscillators (Eq. (2)) diffusively, and expressing the dynamical equations in Cartesian coordinates gives:

$$\begin{aligned} \dot{x}_{1,2} &= P_{1,2}x_{1,2} - \omega_{1,2}y_{1,2} + d(x_{2,1} - x_{1,2}) \\ \dot{y}_{1,2} &= P_{1,2}y_{1,2} + \omega_{1,2}x_{1,2} \end{aligned} \tag{3}$$

with $P_{1,2} = 1 - |z_{1,2}|^2$. The parameter d governs the coupling strength. For $d = 0$, each oscillator has a stable limit cycle at $|z_{1,2}| = 1$ on which it moves at its natural frequency $\omega_{1,2}$, rendering the equilibrium solution of system (3), $z_{1,2} = 0$, linearly unstable. We consider first the case of identical frequencies, i.e. $\omega_1 = \omega_2$, and particularly, without any loss of generality, the case of $\omega_1 = \omega_2 = 2$. To characterize systematically the qualitative changes in the dynamical behavior that occur in parameter space, we perform next bifurcation analysis [62] of the coupled system (Eq. (3)). Here and in the following sections, the results are obtained mainly numerically, using the *Xppaut* package [63]. However, when possible, analytical solutions are also given.

Thus, the bifurcation analysis of the system Eq. (3) has revealed two sets of fixed points: the origin (0, 0, 0, 0) which is unstable, and the pair $(x_{1^*}, y_{1^*}, -x_{1^*}, -y_{1^*})$, where $x_{1^*} = -\frac{\omega y_{1^*}}{\omega^2 + 2dy_{1^*}{}^2}$, $y_{1^*} = \sqrt{\frac{d - \omega^2 \pm \sqrt{d^2 - \omega^2}}{2d}}$. The characteristic eigenvalue equation at the origin determines the conditions for which the nontrivial solution $(x_{1^*}, y_{1^*}, -x_{1^*}, -y_{1^*})$ is stabilized: $d = \frac{\omega^2+1}{2} = 2.5$ [61]. Exactly this solution corresponds to an inhomogeneous steady state or the *OD* phenomenon (Fig. 1).

In general, *OD* is a result of a symmetry breaking of the steady state of the system through a pitchfork bifurcation (labeled PB in Fig. 1a). Thus, the unstable homogeneous state splits into two additional branches which gain stability through Hopf bifurcations, denoted as HB_{s1} in Fig. 1a. This means that the inhomogeneous steady state is manifested through two branches of the stable steady state solution, corresponding to x_1^* and $x_2^* = -x_1^*$ (time series of the corresponding solution are given in Fig. 1b). Moreover, it can be shown that prior to $d = 2.5$, the largest Lyapunov exponent is zero, whereas the second largest is negative, indicating a limit cycle behavior. In particular, two distinct types, in-phase and anti-phase oscillations have been detected in this region [61]. Additionally, an ε-parameter interval can be identified where both, the *IHSS*, as well as the limit cycle coexist. This confirms the statement already noted in the introduction: when the oscillation quenching mechanism belongs to the *OD* type, the phase space is "shared" between the limit cycles and the steady states which coexist.

2.2. Amplitude death

In contrast to *OD*, however, when the quenching of oscillations belongs to the class of amplitude death phenomena, the limit cycle decays towards a central, in this case *homogeneous* steady state, lying within both (for $N = 2$) of the uncoupled limit cycles. To demonstrate this, system equation (3) is again considered. Differently to the previous case however, here the oscillators have a defined frequency mismatch

$$\Delta = \frac{\omega_1}{\omega_2}. \tag{4}$$

Starting from the identical situation ($\Delta = 1$), and increasing the frequency mismatch between the oscillators, first the *OD* loses its stability, rendering only the limit cycle solutions stable [61]. At a critical frequency difference ($\Delta \sim 3.1$) and coupling strength ($d \sim 2.91$), the stability of the origin changes, and the limit cycles collapse into the origin via an inverse Hopf bifurcation (HB_1 in Fig. 2a). This means that the oscillations are quenched under the coupling and the system evolves towards the homogeneous equilibrium which is stable between two Hopf bifurcations, HB_1 and HB_2 (HB_2 occurring for $d = 3.78$ in Fig. 2a). This allows for a stable *AD* effect to be observed: the oscillators pull each other off their limit cycles into the origin, and a *homogeneous* steady state (stable fix point solution, Fig. 2b) emerges, as the classical analysis of oscillation quenching have previously shown [41,50]. However, it was recently shown in [61], that in contrast to classical analysis of *AD*, the pitchfork bifurcation responsible for the symmetry breaking of the *HSS* is still present in a near proximity of HB_2, and right after *AD* is destabilized (PB_1 at $d = 4.48$ in Fig. 2a). Despite the presence of the symmetry breaking bifurcation, the level of heterogeneity in this case permits only *AD* to be observed. Importantly, an additional stable *inhomogeneous limit cycle* emerges from a secondary bifurcation branch stabilized after the pitchfork bifurcation PB_2 (a general description of this solution is given in Section 5.1).

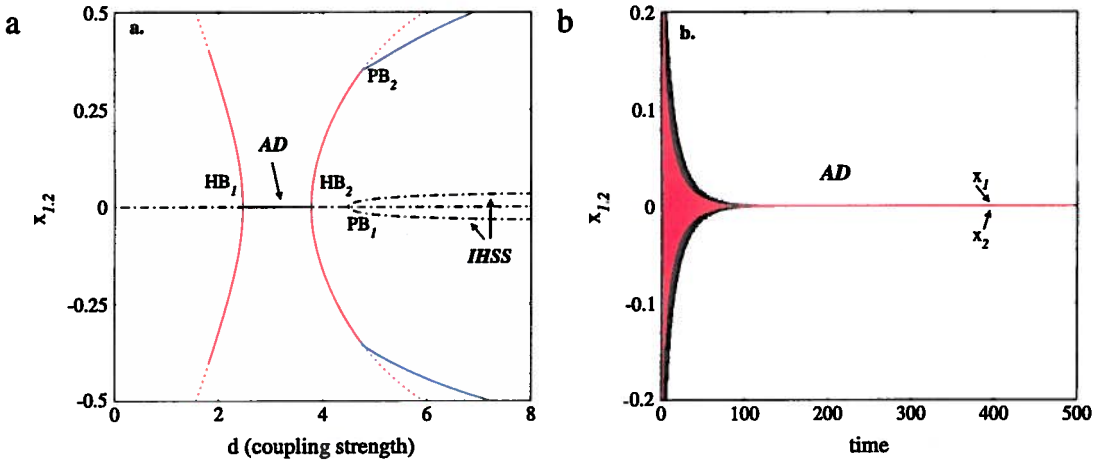

Fig. 2. Manifestation of amplitude death (homogeneous steady state) in System (3). (a) Bifurcation diagram obtained by variation of d, to illustrate the *AD* for $\Delta = 3.25$. Colored (red/blue) solid lines denote stable limit cycles. (b) Time-series representation of *AD* for $N = 2$ coupled oscillators and $d = 3.1$. Different oscillators are represented in different colors. (For interpretation of the references to colour in this figure legend, the reader is referred to the web version of this article.)

We note here that this section serves only to demonstrate the different manifestations of *OD* and *AD* as inhomogeneous and homogeneous steady states. The generation mechanisms that lead to both types of oscillation quenching regimes will be systematically presented in the following sections.

2.3. Turing bifurcation characterizes the transition from AD to OD

Now the question arises: is a transition between both oscillation quenching solutions possible, and if so under which conditions? Following a recent study [61] which addresses this question in detail, the increase of Δ leads to a critical value for which a qualitative changeover occurs: the *AD* phenomenon represented via the stable homogeneous steady state transits to a stable inhomogeneous steady state, or an *OD* regime (Fig. 3). The evolution between these two, very distinct dynamical regimes is characterized with a classical *Turing-type bifurcation*.

This bifurcation scenario is realized as follows: the broken symmetry bifurcation points of the *HSS* and the limit cycle (PB_1 and PB_2 in Fig. 2a) come closer together for increasing Δ, and at $\Delta_{critical} \sim 3.45$ they merge. This gives birth to a supercritical pitchfork bifurcation (PB_1 in Fig. 3) which allows for symmetry breaking of the stable *HSS* (*AD* regime) and a transition to an inhomogeneous steady state and a stable *OD* regime. On the other hand, the supercritical Hopf bifurcation HB_2 which marks the end of the *AD* stability region (Fig. 2a) now moves to the right, resulting in the birth of an unstable limit cycle solution [61]. This bifurcation scenario resembles the key idea underlying the Turing mechanism that a homogeneous equilibrium is stable to homogeneous perturbations, however, far from equilibrium instability can occur, resulting in a

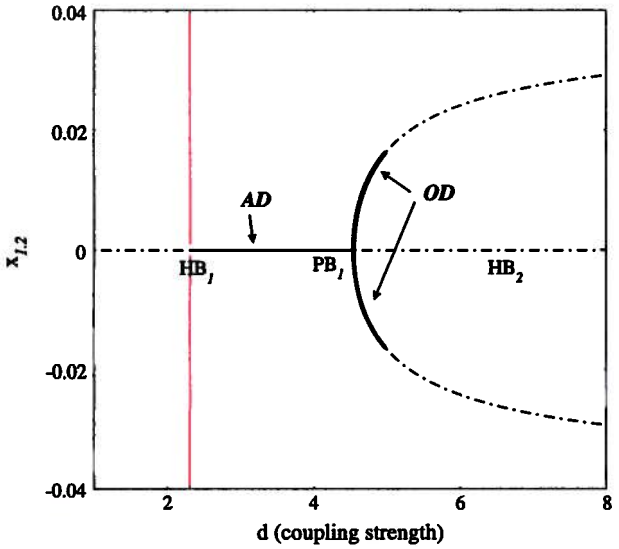

Fig. 3. A classical Turing bifurcation determines the transition from *AD* to *OD*. Above a critical frequency mismatch value, it is possible to observe a transition between *AD* and *OD* phenomena. The colored line (from HB_1) denotes stable limit cycle solution.

time-independent state in which the concentrations are space dependent. Here, the number of oscillators in the system resembles the role of a space variable.

Thus, demonstrating the occurrence and difference in generation mechanisms and manifestation, we underline here the structural distinction between both oscillation quenching types, *OD* and *AD*, which are analyzed in detail in the following sections.

3. Oscillation death: generation principle, characteristics and applications

The idea that the symmetry breaking of the system via a pitchfork bifurcation, as described by Turing in 1952 [46], and mathematically formulated by Prigogine and Lefever [47] for two identical Brusselators coupled in a diffusion-like manner (details of this case will be discussed in Section 3.2.1), has been demonstrated to represent a general dynamical solution in a wide range of coupled systems. It has been shown theoretically that *OD* is model independent, persisting for large parametric regions in several systems of diffusively coupled chemical [64], biological [43,65,44,59,42] or chaotic oscillators [39].

As revealed by experimental studies, the basis for *OD* is a specific, vector-type coupling, namely coupling via a slow recovery variable [8]. Thus, several experimental realizations have shown the existence of *OD* in chemical reactors [40], chemical nano-oscillators (micro-fluidic Belousov–Zhabotinsky-octane droplets) diffusively coupled via signaling species [66], but also electronic circuits [36,37], thermo-kinetic oscillators [52], etc.

This allows *OD* to be considered as a control mechanism of the system's dynamics, with various applications in physics, chemistry, medicine and biology. To that extent, in what follows, we overview the general mechanism of the occurrence of *OD* in paradigmatic classes of coupled oscillators which differ in their structural properties, and coupling characteristics, as well as the size of the observed systems. We note here once again that *OD* in the investigated systems is always accompanied (coexists) in parameter space with stable limit cycle oscillations [8,67,65,44] (and references therein).

3.1. Biological oscillators

Due to the manifestation of the *OD* phenomenon through an inhomogeneous steady state, this oscillation quenching mechanism allows for the formation of heterogeneity in a homogeneous medium. In that context, the idea of oscillation death has been interpreted as a possible mechanism of pattern formation and *cellular differentiation* [46,55,56]. Therefore, the characterization of *OD*, especially in different biological systems is significantly important. This statement is strengthened with the fact that *OD* has been identified as well in neuronal competition models for the description of pattern generators and related to mechanisms for frequency control [54,42].

Next, we characterize the formation and manifestation of *OD* in two general classes of coupled biological oscillators: relaxation and "repressilator" [68] types of oscillators. The dependence of *OD* formation with respect to the oscillator's type, but also the coupling characteristics and network's topologies is overviewed in detail. The results are also generalized for systems of N coupled oscillators, where the main characteristics of *OD* are investigated as well.

3.1.1. Oscillators with an N-shaped nullcline: genetic, calcium and membrane relaxation oscillators

A crucial characteristics of dynamical systems is the positioning of the nullclines: exactly this determines their dynamical behavior. In general, for a system described by first order dynamical equations, i.e. Eq. (1), the nullcline (x_i for example) is

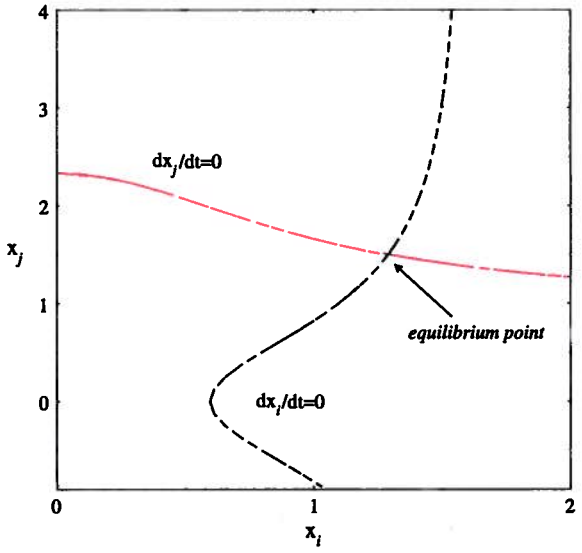

Fig. 4. Overview of system's dynamics (Eqs. (1), (5)): Characteristic N-shaped nullcline for general class of relaxation oscillators. The two nullclines of a general two-dimensional system are represented in different colors. (For interpretation of the references to colour in this figure legend, the reader is referred to the web version of this article.)

the set of points which satisfy

$$F(x_i^j, k) + d_i^j \Sigma(x_i^j - x_i^{j-1}) = 0. \tag{5}$$

Note that the intersection point(s) of all nullclines is an equilibrium point of the system. If the system is characterized with one N-shaped nullcline (N-shaped curve obtained from the condition $\frac{dx_i}{dt} = 0$), and a second one (for $\frac{dx_j}{dt} = 0$) represented as a line intersecting the first one (example given in Fig. 4), an occurrence of alternatively slow and fast "relaxation" oscillations is generated over a wide range of parameter intervals. Thus, a general characteristic of these oscillators is the presence of multiple time scales in the system. Note that time hierarchies are pervasive in biological systems, characterized by a wide separation of time scales of the underlying processes at one and the same level of spatial organization. Thus, fast–slow systems have become one of the major modeling tools for many biological and chemical processes. Here, we use a (synthetic) genetic oscillator [43], a model characterizing calcium (Ca^{2+}) oscillations in the pancreatic β-cells [65], and a membrane oscillator [69] as representative examples. We investigate further the presence of *OD* in the minimal model of two coupled units, and characterize its dependence on the coupling type and the size of the system.

I. *Model of synthetic genetic relaxation oscillators*

In the past several years, collective rhythms of regulatory genetic networks have been a subject of considerable interest, especially because of the fact that the advancement of molecular biology techniques has enabled experimental observations of the dynamics of regulatory networks via engineered synthetic genetic circuits. Therefore, several theoretical [70,71,43,72,59] and experimental models [68,73,74] of distinct synthetic oscillators or populations have been investigated in the literature. The main means of coupling in the constructed systems has been a trans-membrane diffusion of signaling molecules, called autoinducer (*AI*), into an extracellular medium. It has been also shown that a particular realization of an *AI*-mediated coupling in these systems can lead to the appearance of *OD* [43,44,59], only if the *AI* is generated by the slow variable (in contrast to the relaxation model [70] for e.g., where the fast variable regulates the production of *AI*).

I.1 *Globally coupled oscillators*

The model considered here consists of hysteresis-based relaxation genetic oscillators which "communicate" via signaling *AI* molecules [43]. Omitting detailed biological explanations, we focus here on the time evolution of the elements in the system as governed by the dimensionless Eqs. (for a detailed description of the model we refer to [43]):

$$\begin{aligned}
\frac{du_i}{dt} &= \alpha_1 f(v_i) - u_i + \alpha_3 h(w_i) \\
\frac{dv_i}{dt} &= \alpha_2 g(u_i) - v_i \\
\frac{dw_i}{dt} &= \varepsilon(\alpha_4 g(u_i) - w_i) + 2d(w_e - w_i) \\
\frac{dw_e}{dt} &= \frac{d_e}{N} \sum_{i=1}^{N} (w_i - w_e).
\end{aligned} \tag{6}$$

Here, N denotes the total number of cells (oscillators), u_i and v_i represent the proteins which constitute the basis of the oscillator in the i-th cell, and w_i and w_e are the intra- and extra-cellular *AI* concentrations, respectively. The corresponding functions are: $f(v_i) = 1/(1 + v_i^{\beta})$, $g(u_i) = 1/(1 + u_i^{\gamma})$ and $h(w_i) = w^{\eta}/(1 + w^{\eta})$. The dimensionless parameters $\alpha_{1,2,3,4}$ regulate the basic biological operation, and can be, therefore, considered as bifurcation parameters. The coupling coefficients in the system are given by d and d_e (intracellular and extracellular) and depend mainly on the diffusion properties of the membrane, as well as on the ratio between the volume of the cells and the extracellular volume. The presence of two time scales in the model (established for $\varepsilon \ll 1$) allows the system to produce relaxation oscillations which emerge via a Hopf bifurcation ($HB_{1,2}$ in Fig. 5). The structure of the oscillator thus renders w_i to be governed on the slow time scale of the system, whereas u_i, v_i and w_e follow fast dynamics.

Here, we consider the formation of *OD* phenomena with respect to the coupling characteristics. In particular, we overview the properties of *OD* in systems of globally (Eqs. (6)), as well as locally (Eq. (7)) coupled relaxation oscillators. Moreover, the manifestation of *OD* depending on the network topology is also discussed.

To the best of the authors' knowledge, the background mechanism of *OD* is *always* a symmetry breaking instability, which allows for occurrence of an inhomogeneous steady state. Thus, the bifurcation structure of the *OD* phenomena in the system of coupled relaxation oscillators displayed in Fig. 5 resembles the formation of *OD* in the general example of Landau–Stuart oscillators (Fig. 1). Again, the *IHSS* is manifested through two branches of stable steady state solution, which correspond here to two levels of protein concentrations—one of the oscillators populates the upper, whereas the other one the lower branch of the *IHSS*. Moreover, the *OD* coexists in the α_1 parameter space with in-phase oscillations, stable between HB_1 and HB_2 [44].

In the generalized case of N coupled oscillators ($N > 2$), the system (Eq. (6)) demonstrates only two cluster decompositions for *OD*, independent of the number of oscillators. This solution corresponds to the two branches which are born as a result of the *PB* through which the symmetry of the *HSS* of the system is broken: the *OD* is represented as a stable region on the two branches of the *IHSS*, which the N-coupled oscillators then populate. Furthermore, in our previous studies we have observed that for N coupled oscillators, there exist $N - 1$ different distributions of the oscillators between these two stable branches [44,58,75], each characterized by a shift in the protein production level (Fig. 6a). Moreover, each of the $N - 1$ clustering distributions represents a stable attractor with its own basin of attraction, as shown in Fig. 6b using a bifurcation analysis. In Fig. 6b, only the *IHSS* branches are shown for clarity. However, each *IHSS* solution is a result of the symmetry breaking of the steady state of the system via a pitchfork bifurcation, as already discussed.

This means that in a homogeneous population of identical oscillators (cells), *OD* contributes to the formation of a heterogeneous solution. In particular, the cells populate one of the two stable branches, which results in the production of different stable protein concentrations. Differences in the protein concentrations, on the other hand, lead to different cellular functionality, which can be interpreted as cellular differentiation [76,55,56]. Thus, the presence of *OD* in synthetic, and in biological circuits in general, is critical, since it can be considered as a promising tool for cell function regulation: it provides a stable variability of protein concentrations. On the other hand, *OD* can be viewed as an additional mechanism for genetic switching based on interacting limit cycles, a mechanism substantially different from a standard synthetic genetic toggle switch [77]. Fig. 6b demonstrates also the coexistence of the stable attractors characterizing the different *OD* distributions, rendering multistability typical for a system which displays this type of oscillation quenching. This situation is significantly important for biological systems: if one of the regimes becomes unprofitable for cell functioning, the genetic unit can easily switch to some other coexistent regime. Moreover, it has been reported that multistability is a main mechanism for memory storage and temporal pattern recognition [78], fields which could serve as a basis for potential biotechnological applications of the *OD* phenomenon.

I.2 *OD in oscillators locally coupled on a ring*

It is a well known fact that chains (rings) of locally coupled identical oscillators, in contrast to the globally coupled scenario, undergo complicated bifurcation transitions, including the coexistence of multiple periodic orbits with different frequencies and amplitudes, spatial patterns, and modulation instabilities [79–81]. Thus, we discuss here the question whether topologically distinct structures can enhance the dynamical structure of the *OD* phenomenon.

In [82], we have investigated this possibility considering several ring structures of linearly coupled synthetic relaxation oscillators (details of the topology can be found in [82]). In general, these systems can be mathematically represented by substituting the equations for w_i and w_e in the system equations (6) with:

$$\frac{dw_i}{dt} = \varepsilon(\alpha_4 g(u_i) - w_i) + 2d(w_{i+1} + w_{i-1} - 2w_i). \tag{7}$$

Due to the spatial organization of the cells and the diffusive properties of the local, phase-repulsive coupling, *OD* is now manifested via more complex dynamical structures. Hence, in addition to the standard two cluster decomposition, which was initially thought to be the only manifestation of *OD*, different cooperative behavior of the oscillators is possible. The lower (upper) level (or both) can be constituted of several sub-clusters, characterized with different protein expression levels. Fig. 7a, b shows here two possible examples: in the case of $N = 16$ identical oscillators, the occurrence of *OD* e.g. in the form of 2 vs. 4, as well as 4 vs. 4 cluster decompositions is possible, with different distributions of the oscillators between the stable attractors (stable with respect to small perturbations). However, as already noted, the local coupling contributes to the stabilization of a large number of attractors, thus, the systematic classification of the various *OD* manifestations for N locally coupled oscillators awaits further analysis.

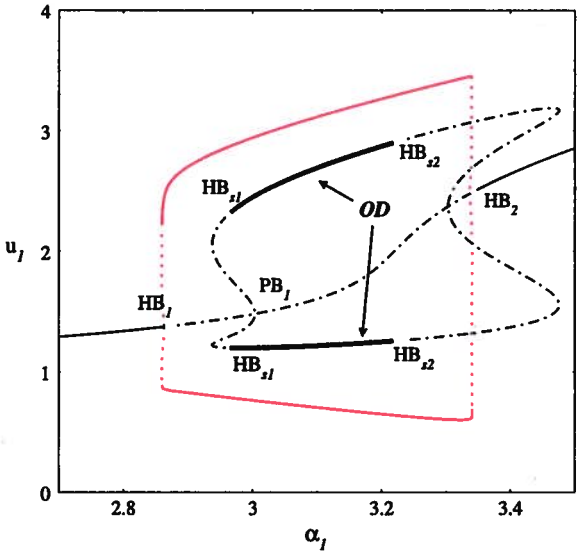

Fig. 5. Bifurcation diagram obtained by variation of α_1 to illustrate the *OD* in a system of $N = 2$ coupled identical genetic oscillators (System (6)). Thick solid lines denote stable *OD*, whereas solid colored line (between HB_1 and HB_2) represents stable in-phase oscillations. Parameters: $\varepsilon = 0.01$, $\alpha_2 = 5$, $\alpha_3 = 1$, $\alpha_4 = 4$, $\beta = \eta = \gamma = 2$, $d = 0.01$ and $d_e = 1$.

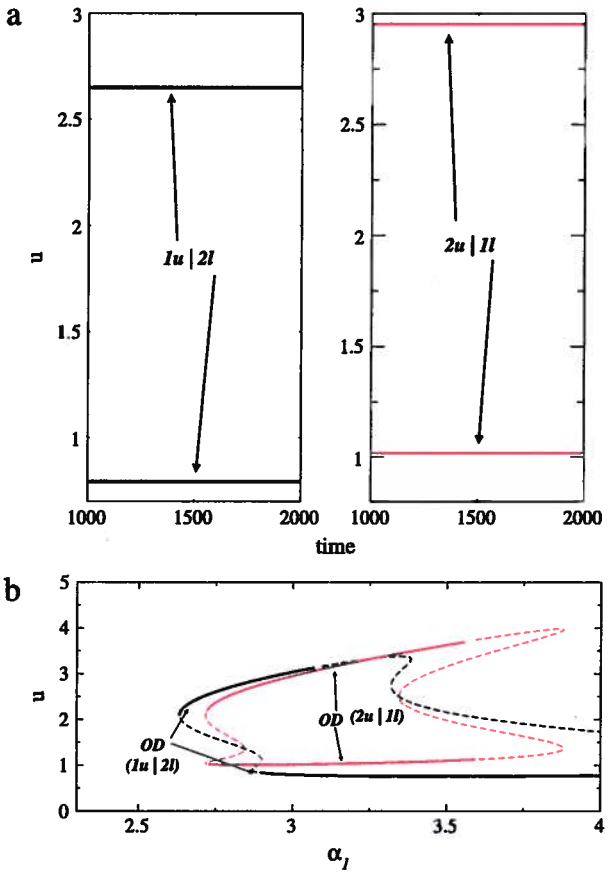

Fig. 6. (a) Examples of different distributions in the *OD* regime for $N = 3$ identical oscillators. $d = 0.3$ and other parameters as in Fig. 5. Distribution (i) 1:2, where one oscillators occupies the upper level, and two oscillators the lower one; (ii) 2:1 distribution. Note the different protein levels for different oscillator distributions. (b) Bifurcation structure of the two stable distributions of the oscillators in the *OD* branches. Different colors correspond to different stable *IHSS* attractors. Other parameters as in Fig. 5.

This novel type of *OD* manifestation which we discussed in [82] for the first time, can play a crucial role in biotechnological applications. One could envision a new synthetic design based on the currently investigated network properties in order to

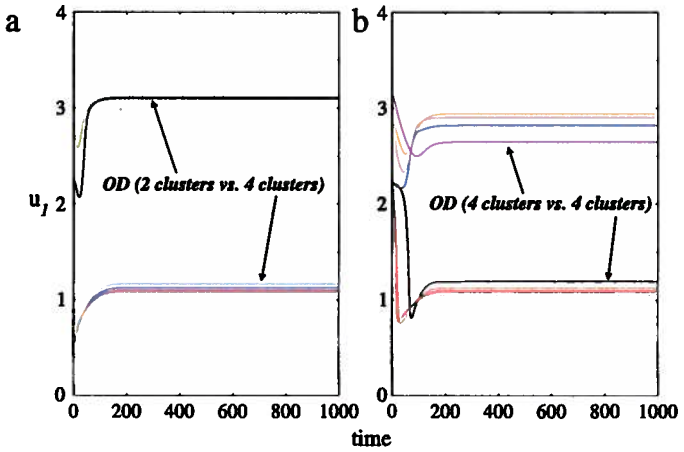

Fig. 7. Novel *OD* manifestation as a (a) 2 vs. 4 cluster decomposition (distribution of the oscillators between the clusters (4:4) vs. (2:2:2:2)) and (b) 4 vs. 4 cluster decomposition (oscillator distribution (3:1:2:2) vs. (1:2:2:3)) for a system of $N = 16$ locally coupled relaxation genetic oscillators (Eq. (7)). Within the clusters the oscillators exhibit identical behavior. Different clusters are denoted in different colors. Both distributions represent stable attractors [82]. (For interpretation of the references to colour in this figure legend, the reader is referred to the web version of this article.)

construct small synthetic units to serve as efficient memory devices, offering enhanced storage capabilities (depending on the number of sub-clusters present) in contrast to the contemporary memory devices.

Based on this, we can state that the *OD* phenomenon has significantly different characteristics in globally and locally coupled systems (note that qualitatively similar behavior will be observed for various models of locally coupled relaxation oscillators). We underline here in particular the non-standard manifestation of *OD*, where separate stable clusters are additionally characterized with the formation of sub-clusters. Again, there exists a possibility for different oscillator distributions between separate (sub)clusters, which in turn leads to multiple stable attractors and a very complex dynamical structure in systems of identical oscillators, locally coupled on a ring.

II. *OD in models of calcium and membrane oscillators*

The study of *OD* can contribute as well to the understanding of various other biological phenomena. We demonstrate here two case studies: the problem of Ca-metabolism in insulin-secreting pancreatic β-cells (Eq. (A.1)) [65], and a model of membrane oscillations used to describe the kinetics of lipid peroxidation in a cell membrane (Eq. (A.2)) [83,69]. Both oscillators are of relaxation type characterized with N-shaped nullclines, similarly to Fig. 4.

(i) An important control center in the glucose homeostasis is the insulin-secreting pancreatic β-cell, localized in the Islets of Langerhans. Insulin secretion is a complex multicellular process, which relies on the interaction between β-cells within an islet, as well as on the interactions between islets in the pancreas. Under normal conditions, glucose stimulation evokes well-synchronized oscillations of the cytosolic Ca^{2+} concentration ($[Ca^{2+}]_i$) in the β-cells in an islet, which in turn triggers pulses of insulin secretion [84,85]. It has been suggested that a disturbance in the Ca^{2+} oscillations could contribute to the irregularity of insulin oscillations in diabetes patients. Therefore it is of utmost interest to investigate and characterize the mechanism underlying the disruption or suppression of Ca^{2+} oscillations in this case.

The dynamical behavior of this system using a Morris–Lecar-like β-cell model (Eqs. (A.1)) was investigated in the regions of strong [65] and moderate coupling [58] and shown that in the case of identical cells, symmetry breaking in the system allows for classical *OD* to be observed. However, this oscillation quenching regime coexists over the full parameter range with synchronous oscillations which are a necessary precondition for proper insulin secretion (Fig. 8a). This means that the diffusion of calcium through gap junctions, if too strong, can have a de-synchronizing effect by promoting *OD*, from which it was concluded that Ca^{2+} gap-junctional diffusion does not make an important contribution to the normal function of pancreatic Islets of Langerhans.

(ii) The membrane model (Eq. (A.2)) used to describe the kinetics of lipid peroxidation in a cell membrane, and also interpreted as a model for the cell cycle of mammalian cells [83,69] is another strong relaxation oscillator generating a limit cycle due to an N-shaped nullcline. The phase portrait of this model is in general very similar to the structure of the synthetic genetic oscillator discussed previously (Eq. (6)). However, due to its biological relevance, a different coupling type, namely *local coupling* via the slow variable seems more appropriate here. The occurrence and manifestation of *OD* for identical oscillators is qualitatively the same as in the previously considered examples (Fig. 8b). Moreover, for any value of the coupling coefficient for which *OD* is present in the system, there is a clear coexistence of the *OD* regime with the full amplitude oscillatory regimes (limit cycle solution between HB_1 and HB_2 in Fig. 8b).

Thus, we can conclude that in systems of coupled relaxation oscillators, *OD* is *always* a result of a symmetry breaking of the system via a pitchfork bifurcation. The two branches of the *IHSS* which occurs in this case are further stabilized via Hopf bifurcations. Moreover, distinct topological structures can give birth to more complex *OD* regimes: lower (upper) level (or both) can be constituted of several sub-clusters [82]. However, we have to emphasize here the fact that the manifestation of the *OD* phenomenon in chains of locally coupled oscillators is not exploited in full detail and awaits further investigations.

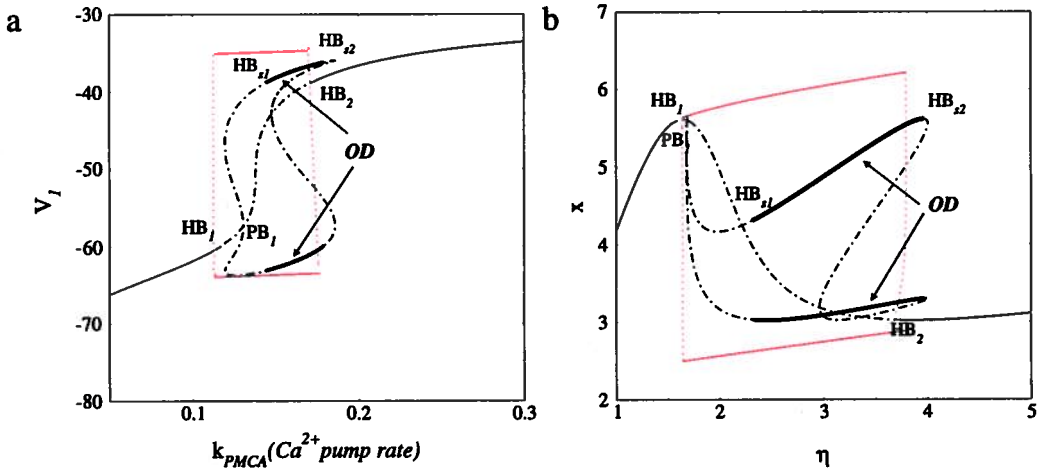

Fig. 8. Manifestation of: (a) coexistence of *OD* and limit cycle oscillations (red lines) for a system of $N = 2$ coupled identical Morris–Lecar-like β-cells (Eq. (A.1)) for coupling coefficient $g_{c,Ca} = 0.05$; and (b) coexistence of *OD* and limit cycle oscillations for a system of $N = 2$ coupled identical membrane oscillators (Eq. (A.2)) with coupling strength $d = 1.0$. The remaining parameters are the same as in [58] (For interpretation of the references to colour in this figure legend, the reader is referred to the web version of this article.)

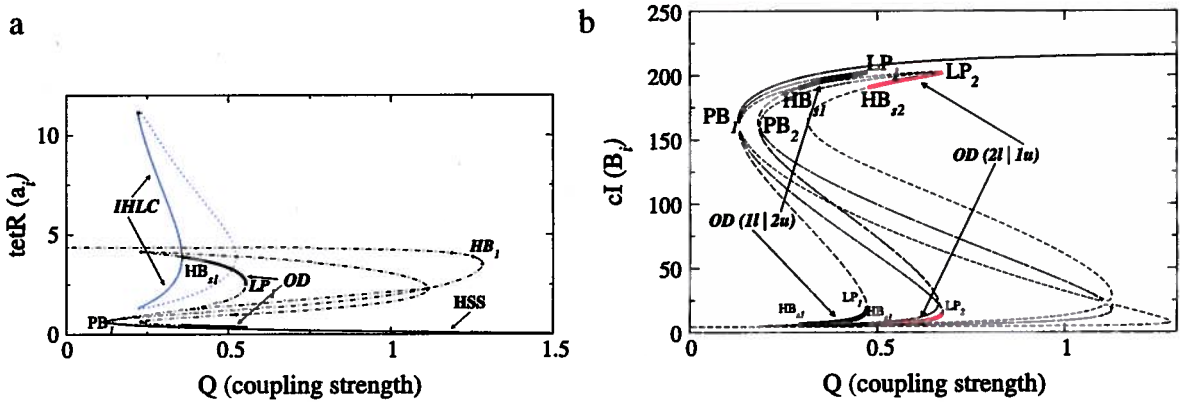

Fig. 9. Manifestation of: (a) *OD* for a system of $N = 2$ coupled identical repressilators. The *HB* on the boundaries of *OD* results in stable *IHLC* oscillations (blue lines); and (b) clustering in the *IHSS* regime for $N = 3$. The figure is reproduced with parameters from [86]. (For interpretation of the references to colour in this figure legend, the reader is referred to the web version of this article.)

3.1.2. Emergence of OD in system of coupled repressilators

Despite relaxation, phase oscillators constitute a significant modeling tool to study various physical or biological systems [68]. In order to demonstrate the existence and manifestation of *OD* in this class of systems, we use a well-studied model of a synthetic oscillator termed a *repressilator* and developed in *Escherichia coli* from a network of three transcriptional repressors (*tetR*(*A*), *cI*(*B*), and *lacI*(*C*)) that inhibit each other in a cyclic way [68]. The coordinated behavior of a population of coupled oscillators and its transition to synchrony was studied through the influence of a chemical coupling (quorum-sensing mechanism realized via *AI* signaling molecules) [71], whereas a slight modification of the coupling mechanisms leads to the presence of various dynamical regimes [59].

In contrast to the relaxation oscillators, where *OD* results from the symmetry breaking of the unstable steady state, in the model of coupled repressilators (Eq. (A.3)), the situation is slightly different: the pitchfork bifurcation which results in the *IHSS* is born here from a *stable* steady state (Fig. 9a). Moreover, the boundaries of the stable *IHSS* are not obligatory Hopf bifurcations (as in Figs. 5, 8), but stable *OD* can be marked as well with saddle–node bifurcations (LP_1 in Fig. 9a). The model system (Eq. (A.3)) possesses another very important characteristic: *OD*, or more precisely, the boundary supercritical Hopf bifurcation of stable *OD* gives birth to a stable limit cycle, the so-called inhomogeneous limit cycle (*IHLC*, discussed in detail in Section 5.1) [86].

Therefore, the phase space is now "split" between the *HSS*, the *IHSS* and two different limit cycles, an *IHLC* (born from HB_{s1} in Fig. 9) and anti-phase oscillations emerging from HB_1 (the stable limit cycle emerging from HB_1 is not displayed in the figure for improved clarity). Moreover, for N coupled oscillators, $N - 1$ different distributions between the 2-cluster decompositions of *IHSS* are again possible, similarly to the situation described in Section 3.1.1. Let us define the different cluster states by the notation $ml|(N - m)u$, which denotes a cluster of m oscillators in the low-protein concentration state l, while the remaining $N - m$ oscillators populate the upper state u, characterized by higher protein concentration. In [55] we have determined the following dependency: clusters of the type $1l|(N - 1)u$ require small coupling values Q, while the

$(N-1)l|1u$ exist for large Q (Fig. 9b). Each possible partition, as in the case of relaxation oscillators, shows slightly different levels in the protein concentrations, and hence, a fine tuning of the protein levels can be accomplished by choosing a specific coupling interval for proper partition of the oscillators.

3.2. Chemical oscillators

The problem of coupling two chemical oscillators was first dealt with by Prigogine and Lefever [47] who showed that two Brusselators, when coupled in a diffusion-like manner can break symmetry and arrive at the *IHSS*, setting therefore the ground work on the *OD* phenomenon (a brief description of the proof is given in Appendix A.4). Bar-Eli later on extended this study by discussing the formation of *OD* in systems of N coupled identical, as well as almost identical Brusselators [64].

The first experimental results on *OD* were however reported by Dolnik and Marek by demonstrating the extinction of oscillations in chemical reactors coupled by mutual mass exchange [40]. Later, Crowley and Epstein investigated the Belousov–Zhabotinsky reaction in stirred tank reactors coupled by mass flow and showed that the basis for *OD* is a specific, vector-type coupling, namely coupling via the slow recovery variable of the system [8]. Moreover, they showed experimentally the existence of all dynamical regimes and the relations between them, i.e. the coexistence of *IHSS* and in-phase oscillations, as we have shown for various biological systems in the previous section. Similar experimental observations were also made in [87]. Moreover, the existence of *OD* was also shown for different models of chemical oscillators, such as the Field–Körös–Noyes model [88], as well as observed experimentally in chemical nano-oscillators (micro-fluidic Belousov–Zhabotinsky-octane droplets) with diffusive coupling [66].

In what follows, we overview the mathematical formalism and the manifestation of the *OD* phenomenon in systems characterized with model-specific phase portraits, i.e. Brusselators, Oregonators and chemical droplets.

3.2.1. Oscillators with model-specific phase portraits

In this section we investigate conditions necessary for the emergence of *OD* in systems which differ in their dynamical structure from the previously investigated oscillators with N-shaped nullclines. In particular, we consider two chemical models, the well-known Brusselator model and a model describing the Belousov–Zhabotinsky (*BZ*) reaction (using a simplified Oregonator model (Eqs. (A.5)) and a model of chemical droplets), both characterized with specific phase portraits. In general, the Brusselator has a particular triangle-like phase portrait (Fig. 10a), with three distinct times (or rates) on the cycle: T_{slow} (T_{12}) being the time of a phase point motion on the slow (left) part of the x-nullcline, the time of jump to the y-nullcline is denoted as T_{fast} (T_{23}, T_{41}), and $T_{moderate}$ (T_{34}) characterizes the time of motion of the phase point on the y-nullcline. The relaxation of the oscillators is defined as: $T_{slow}/(T_{fast}+T_{moderate})$. On the other hand, the Oregonator model has a more specific structure of the phase portrait, marked by the coexistence of homogeneous and inhomogeneous steady states [58]. In contrast to the models describing the oscillators with an N-shaped nullcline which contain the parameter ε in an explicit form, the stiffness in these two models is controlled by the kinetic parameters. In what follows, we analyze in detail the conditions necessary for the appearance of *OD* separately in both systems.

I. *Model of diffusively coupled Brusselators*

The Brusselator is an autocatalytic model involving two intermediates (the general form is described by Eq. (A.4).). It illustrates how the fundamental laws of thermodynamics and chemical kinetics as applied to open systems far from equilibrium can give rise to self-organizing behavior and dissipative structures in the form of temporal oscillations and spatial pattern formation. In the simplest form, the Brusselator model includes two coupled variables representing the concentrations of the intermediate products. Thus, the classical model for two identical Brusselators with vector coupling (via y) through a semipermeable membrane is described by:

$$\begin{aligned}\frac{dx_i}{dt} &= A-(B+1)x_i+x_i^2y_i\\ \frac{dy_i}{dt} &= Bx_i-x_i^2y_i+d(y_j-y_i)\end{aligned} \tag{8}$$

with x_i and y_i being the phase variables, and A, B the system's parameters. The point $x_{1,2}=A, y_{1,2}=B/A$ defines the steady state of the system. Evaluating the eigenvalues of the Jacobian at this point, we get that $Re\,\lambda_{1,2}=0$ for $B=A^2+1$, and $Re\,\lambda_{3,4}=0$ for $B=A^2+1+2D$, following that a Hopf bifurcation occurs when two of the complex conjugate eigenvalues cross the imaginary axis. Furthermore, when $\lambda_4=0$ for $B=A^2/2D+1$, a pitchfork bifurcation (PB_1 in Fig. 10b) occurs, defining branch switching points: the one of the origin ($x_{1,2}=A, y_{1,2}=B/A$) and the inhomogeneous steady state (*IHSS*), which is symmetric to the interchange ($x_1, y_1 \leftrightarrow x_2, y_2$), and is therefore double degenerate [89,67].

Characteristic for this system, similarly to the repressilator case, is the existence of a stable inhomogeneous limit cycle from the HB_{s2} which determines the boundary of the *IHSS* (Fig. 10b). Moreover, it was shown that in the general case of N coupled Brusselators [64,58], the manifestation of *OD* does not change: the oscillators populate the upper or the lower level of the *IHSS*, with a possibility for different distributions of the oscillators between the two stable branches.

II. *Model of coupled BZ-oscillators: oregonators and chemical droplets*

One of the most frequently used models to investigate the dynamics of chemical systems is the model constructed from two, nearly identical Belousov–Zhabotinsky (*BZ*) oscillators. In most of the cases, this setup usually includes large reactors

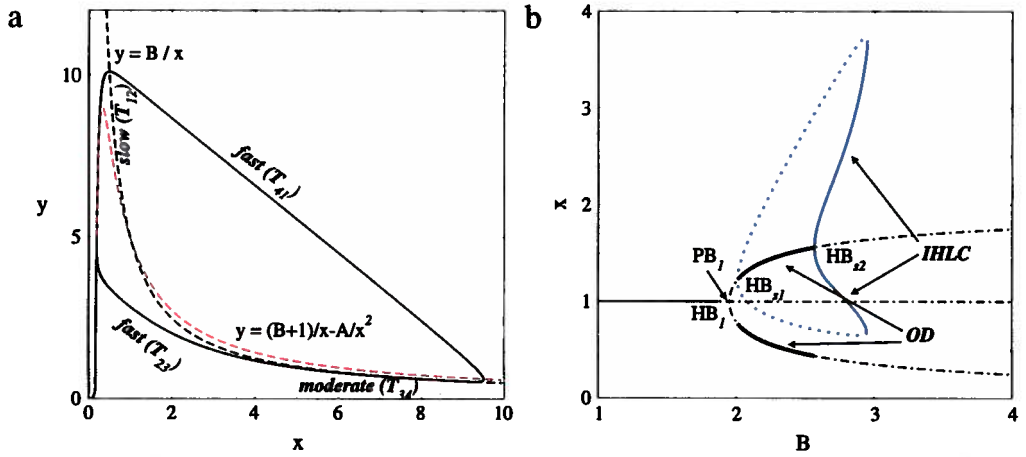

Fig. 10. (a) Nullcline representation (dashed lines) in a triangle limit cycle (Brusselator model, Eq. (8)); and (b) *OD* realization for two identical Brusselators. The *HB* that stabilizes the *OD* solution gives birth to an *IHLC* denoted with blue lines. Parameters as in [58].

connected directly by small channels for controlled mass exchange of bulk solution. One manifestation of such a system is given through a 3-variable Oregonator model (Eqs. (A.5)), used in [8] to elucidate how the chemistry of the system generates the various behaviors (such as *OD*, in-phase and anti-phase oscillations) observed in experiments. In the case of identical elements, the bifurcation diagram is a non-standard one compared to the systems with an *N*-shaped nullcline. Here, in a large part of the parameter interval, there is a coexistence of *OD* with the stable steady state of the system, and an additional coexistence with the in-phase oscillations [58].

In living systems, however, coupling often occurs through signaling molecules, as a synaptic communication (excitatory or inhibitory) or chemotaxis [90]. To mimic such distinct communication scenarios in chemical systems, micro-fluidic devices have been used [66]. In particular, the experimental construct consists of a linear array of droplets of very small volume containing a *BZ* solution separated by octane drops in a glass capillary. This allows the characteristic time of, here inhibitory communication, to be smaller than the period of the oscillations.

This type of systems are significantly important for the investigation of *OD* phenomena, since they inevitably resemble biological systems (in particular the type of systems that were discussed in Sections 3.1.1(I) and 3.1.2). Here, the clear analogy of the chemical droplets to living cells, each containing separate oscillators, can be established. However, in contrast to cellular populations, these systems allow an efficient control of the characteristic time of diffusion. Moreover, the individual dynamical behavior of each droplet can be observed. Thus, by changing the concentration of one of the constituents of the *BZ* oscillators, the authors in [66] observed the formation of a *stationary Turing pattern*, which is in general the classical *OD* regime. As reported in this work, the transition to *OD* goes through intermediate anti-phase oscillations, or almost immediately, depending on the concentration of the phase variable which is experimentally manipulated.

3.3. Chaotic oscillators

The investigations of coupled chaotic oscillators have been generally focused on synchronization transition scenarios (i.e. phase, lag and complete synchronization [91] or anti-phase synchronization [92]), whereas the possibilities of oscillation quenching have been limited to the case of amplitude death, or the disappearance of oscillations and the transition to a stable homogeneous fixed point [93–95,38]. It is only recently that the conditions for *OD* in systems of coupled chaotic oscillators have been addressed [96,39], in particular by studying linearly coupled identical chaotic oscillators without time delay, such as the Lorenz system (A.6) or coupled Pikovsky–Rabinovich (*PR*) oscillators (A.7) [97].

In [39] it was shown that the transition to *OD* is model-dependent, i.e. Lorenz oscillators have to be coupled by conjugate or negative coupling, whereas standard diffusion of one component is sufficient for a pair of *PR* oscillators to exhibit *OD*. In order to demonstrate the general principles of *OD* occurrence in systems displaying chaotic behavior, we overview next a specific case of dissimilarly coupled identical Lorenz oscillators as given in Eq. (A.6). For a given parameter set, the coupled system is characterized, among others, with non-symmetrical equilibrium $A_{1/2}$ and A_3, which is the basis for the occurrence of *OD* as the coupling coefficient moves from zero (Fig. 11a). For further details on the *OD* solutions in the system of coupled Lorenz oscillators we refer the reader to [39].

The *OD* is here stable between a subcritical Hopf and a transcritical bifurcation (*TB* in Fig. 11a), and it resembles the manifestation observed and extensively discussed previously: one of the coupled Lorentz oscillators populates the upper, whereas the second oscillator populates the lower stable branch of the *OD* solution.

Moreover, in systems of coupled chaotic oscillators the transition process to *OD* is also interesting to study. In particular, for the case of Lorenz oscillators described here (Eq. (A.6)), before *OD* is stabilized the system is characterized with an asymmetrical chaotic regime with laminar intervals of synchronous chaos. On the other hand, for a slightly different coupling matrix (via the *x* variable), the system transits from a symmetrical chaos regime to a non-symmetric limit cycle, then to a

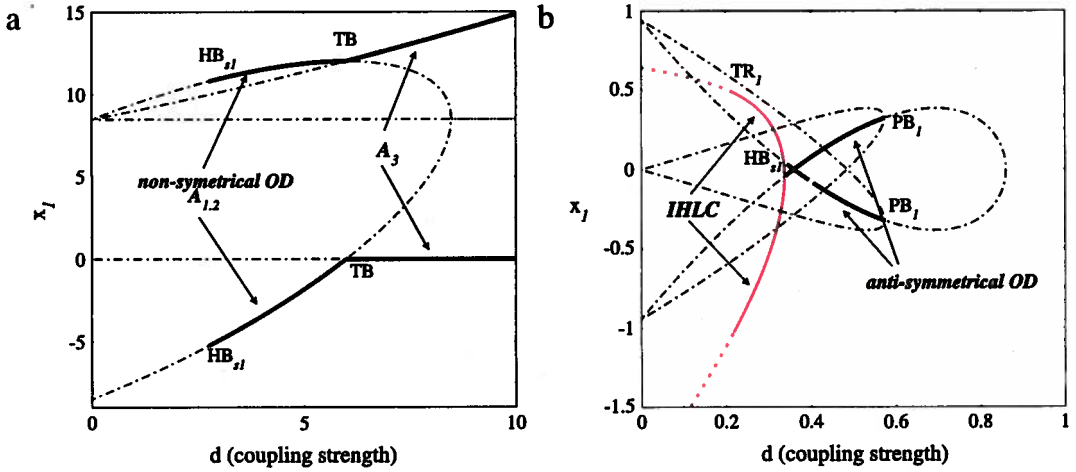

Fig. 11. (a) Manifestation of *OD* in system of coupled Lorenz oscillators (A.6). (b) Stable *OD* and *IHLC* in system of coupled Pikovsky–Rabinovich circuits (A.7).

non-symmetric quasi-periodic regime, and finally to the coexistence of anti-phase synchronization and a quasi-periodic regime until *OD* is stabilized via a Hopf bifurcation [39]. These nontrivial transitions from chaotic dynamics to an oscillation quenching state, and in particular the one of *OD*, thus opens valuable possibilities for chaos control applications that need to be further exploited.

It is also important to note here observations of *OD* for the system of coupled Pikovsky–Rabinovich circuits (Eqs. (A.7)) due to its remarkable analogy with the dynamics of coupled periodic elements. Interestingly, in this case, the coexistence of *OD* with synchronous chaos has been established [39], similarly to our previous observations of *OD* in general systems, as presented in Sections 3.1–3.2. Moreover, analogously to the case of coupled repressilators (Eqs. (A.3)) or Brusselators (Eqs. (8)), where the *HB* which stabilizes *OD* gives rise to a stable *IHLC* solution, here the anti-symmetrical *OD* (stable between a Hopf and a pitchfork bifurcation, HB_{s1} and PB_1 in Fig. 11b) transits to an inhomogeneous limit cycle (stable between HB_{s1} and a torus bifurcation TR_1 in Fig. 11b), and then to inhomogeneous chaos with decreasing coupling strength d. Thus, the manifestation of *OD* (and *OD*-related regimes) in systems of coupled chaotic oscillators provides a rich dynamics which deserves detailed future investigations.

3.4. Neuronal oscillators

Recent studies of firing-rate models for neuronal competition, as observed in binocular rivalry and central pattern generators [54,42], have investigated the importance and physiological meaning of oscillation quenching mechanisms. Although the framework for neuronal competition initially appeared in the descriptions of neuronal development, it has been further applied in the modeling of various neuronal computational tasks, resulting in the detection of the oscillation death phenomenon, termed in the neuroscience literature as *"winner-take-all"* behavior. In neuronal systems, this behavior represents the state when one (sub)population remains active, whereas the other one is indefinitely inactive as a result of the inhibitory interactions, so the switching between states does not take place any longer. Exactly this type of behavior has been previously proposed in the literature as a model for a short term memory and attention [98], or for the selection and switching in part of the basal ganglia under both normal and pathological conditions [99,100].

The mechanism of occurrence of *OD* in neuronal models follows the classical bifurcation scenario that we have described so far: symmetry breaking of the unstable homogeneous steady state of the system (via a pitchfork bifurcation, *PB* in Fig. 12) leads to the appearance of an inhomogeneous steady state, further stabilized via Hopf bifurcations ($HB_{s1,s2}$ in Fig. 12) [54,42]. Here, we demonstrate this behavior on a minimal model of two inhibitory coupled cells, with a slow process in the form of spike frequency adaptation and/or synaptic depression, (Eq. (A.8)) that respond to two competing stimuli of equal strength, as shown in (Fig. 12).

The winner-take-all behavior, or the *OD* may persist for a long time in a neuronal population. However, this might not be indefinite, if some mechanism for slow fatigue or adaptation is present. It is important to note, however, that *OD* in neuronal systems appears both as a consequence of changes in the inhibition strength (an internal parameter of the system) [101], as well as in the case presented here—due to changes in the stimulus strength [54]. However, it is necessary to underline the fact that *OD* in neuronal systems has been observed for non-diffusive coupling, in contrast to the observations made in the examples presented previously in this review.

Even though the theoretical characterization of *OD* for neuronal systems is obvious, the evidence for its direct relation to physiological behavior, such as the one proposed for short-term memory for example, is currently limited and speculative. It will be therefore of significant interest to consider this dynamical solution and its importance for the characterization and manifestation of different physiological conditions in future.

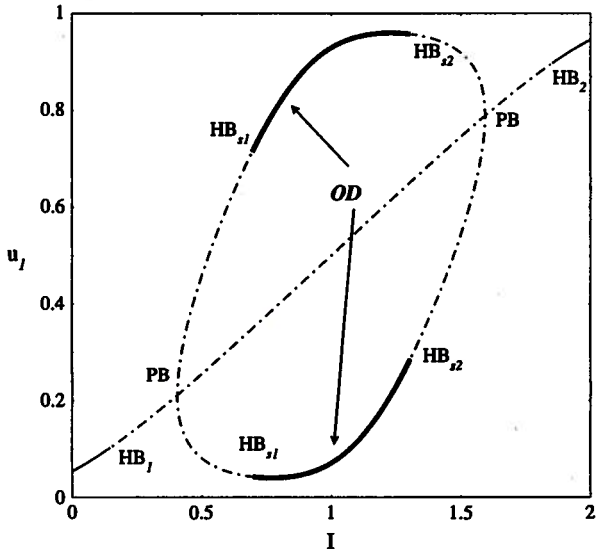

Fig. 12. Manifestation of *OD* in system of coupled identical neuronal oscillators (Eqs. (A.8)) when the external stimulation I is varied. Thin solid lines represent homogeneous steady state, thick solid lines—*OD*, whereas dash-dotted lines represent unstable steady state. The figure is reproduced with parameters from [42].

4. Oscillation death dominance: role of parameter mismatches

In the previous sections we have discussed extensively the fact that the phase space of systems of linearly-coupled oscillators is "split" between limit cycles and inhomogeneous steady state, that is the regions of stability of *OD* and different oscillatory solutions (i.e. in-phase oscillations) always coexist. Considering however, that *OD* can be regarded as a stabilization criteria in systems of coupled chaotic oscillators [39], or it can be directly related to distinct biological phenomena [65,42,55], it is important to discuss under which conditions an *OD* solution will dominate the parameter space. To that extent, we have established in [57] that detuning can abolish limit cycle oscillations, and replace them with *OD* at a certain appropriate magnitude of the coupling strength, a phenomenon which we termed *"oscillation death dominance (ODD)"*. In what follows we overview the basic characteristics of this effect.

We consider next the case of coupled genetic relaxation oscillators described with Eq. (6), with the seeming difference to Section 3.1.1: here, it is assumed that detuning between different oscillators exists, expressed in the variability of the α_1-parameter values as:

$$d_{ij} = \frac{\alpha_1^{(i)}}{\alpha_1^{(j)}}. \tag{9}$$

As a result of the detuning present in system (Eqs. (6) and (9)), the *HSS* corresponding to cells being identical (Fig. 13a), here splits into slightly different steady states with different protein concentrations which both coupled oscillators populate (Fig. 13b). Moreover, the presence of even a 4% difference between the distinct cells leads to a destabilization of the limit cycles in the parameter region where *OD* is stable: the detuning abolishes completely the oscillatory solutions in a large part of the parameter plane, replacing them completely with *OD* for critical values of the coupling strength (Fig. 13c). The detailed relation between the detuning (d_{ij}) and the coupling parameter (d) for the occurrence of *ODD* is given in [57]. The limit cycle which is now stabilized between the Hopf bifurcations of the stable homogeneous and inhomogeneous steady states is the branch of the asymmetric oscillations, allowing the dominance of the *OD* regime to be established (Fig. 13c).

The effect of *ODD* is rather general and valid for systems where global intensive inhibitor diffusion takes place. It has been shown to exist for multiple systems that exhibit the *OD* phenomenon (in particular, for all of the systems discussed in Sections 3.1.1–3.2) [58]. Moreover, the particular detuning dependent dominance of *OD* demonstrates once more the difference between the *OD* and *AD* regimes, since disorder of frequency dispersion has been shown to eliminate *AD* [102]. Additionally, if we consider that *OD* can be interpreted as an extension of Turing's mechanism in oscillatory media (although the phase space is shared with a limit cycle), then it can be stated that *ODD* enlarges the robustness of the Turing structures in oscillatory media. Furthermore, *ODD* provides an additional parameter, the value of detuning, as a controlling mechanism for the transitions between steady and oscillating states in developing, in particular, in biological systems.

5. OD-related regimes

The symmetry breaking phenomenon resulting in the emergence of an *IHSS* as described here is not only characteristic for steady state solutions. In particular, after the existence of *IHSS* was shown for two identical coupled Brusselators [47], Tyson

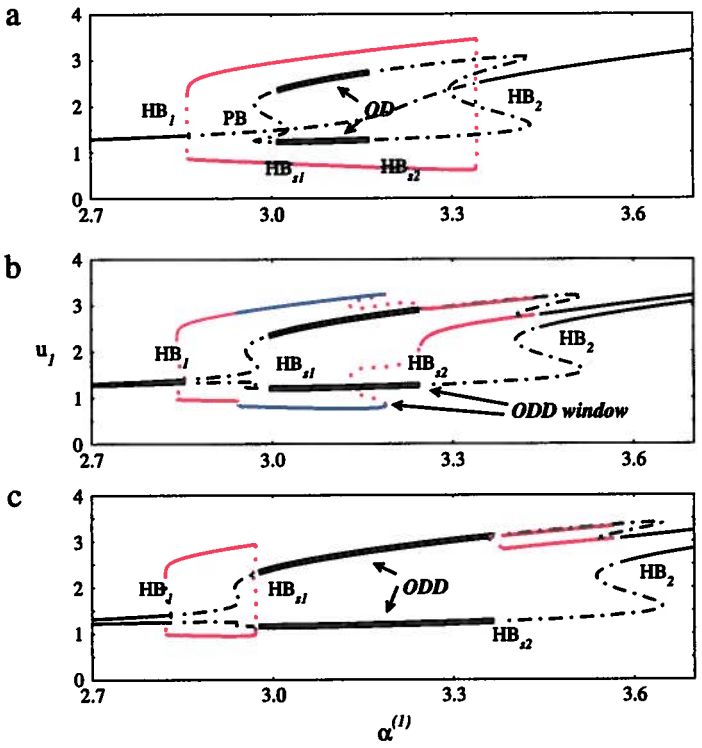

Fig. 13. The effect of *ODD*: *OD* dominates the phase space in system of coupled genetic oscillators (Eqs. (6) and (9)). (a) In the case of identical oscillators, *OD* and limit cycle (red line) share the phase space ($d = 0.008$, $d_{ij} = 1$). (b) Presence of detuning between parameters starts removing the limit cycles (red and blue lines) from the region where *OD* is stable, thus allowing a stable *ODD* window for $d_{ij} = 0.98$, whereas (c) increased detuning, i.e. $d_{ij} = 0.95$ allows for complete dominance of *OD* in parameter space. The limit cycles (red lines) are pushed to the sides of *OD*. Other parameters as in Fig. 5. (For interpretation of the references to colour in this figure legend, the reader is referred to the web version of this article.)

and Kauffman discovered a spatially inhomogeneous limit cycle (*IHLC*) [89]. Additionally, complex spatiotemporal behavior was observed near the stability boundaries of inhomogeneous steady states in the form of mixed-mode oscillations [103,42] and partial oscillation death [82]. In the following we overview the main characteristics of these dynamical regimes and their relation to the existence of a stable *IHSS* solution (*OD*).

5.1. Inhomogeneous limit cycles

The inhomogeneous limit cycle is defined as a periodic solution of a system of coupled oscillators rotating around two spatially nonuniform centers (Fig. 14a). It emerges from the Hopf bifurcation of the inhomogeneous steady state and if this Hopf bifurcation is supercritical, then the *IHLC* is stable (stable *IHLC* are shown in Figs. 9a, 10b) [89,67,86,55]. Contrary to oscillators with an *N*-shaped nullcline, the system of two coupled Brusselators or repressilators, for example, easily demonstrate a spatially inhomogeneous limit cycle with high frequency oscillations and amplitudes very sensitive to the coupling.

Furthermore, for increased size of the system, the parametric region where both inhomogeneous solutions (steady state and limit cycle) are stable is significantly increased at the expense of the *HSS* (the relation between stable *IHSS* and the size of the system we already discussed in detail in the previous sections). The reason for this is the clustering that occurs, and in the case of the *IHLC*s, the oscillators exhibit identical behavior within a single sub-cluster, but with various phase relations among them. The number of oscillators in a given cluster also affects the amplitude and period of the *IHLC* oscillations [55]. This means that the presence of an *IHLC* has as a consequence a well pronounced multirhythmicity in the system, and can be seen as an additional mechanism of generating heterogeneity in initially homogeneous systems. Exactly this property of the inhomogeneous dynamical solutions is crucial for biological systems and has been further related to cellular and stem cell differentiation [55,56].

5.2. Mixed-mode oscillations

In systems characterized with fast and slow dynamics and for a certain range of control parameters, the *IHSS* can transit to a mixed-mode regime [103,42]. In general, the mixed-mode oscillations are defined as complex oscillatory patterns consisting of small-amplitude high-frequency oscillations that alternate with the single large-amplitude long-period cycle (Fig. 14b) [104–107,42]. The parametric area of stability of the mixed-mode oscillations depends on the stiffness of the

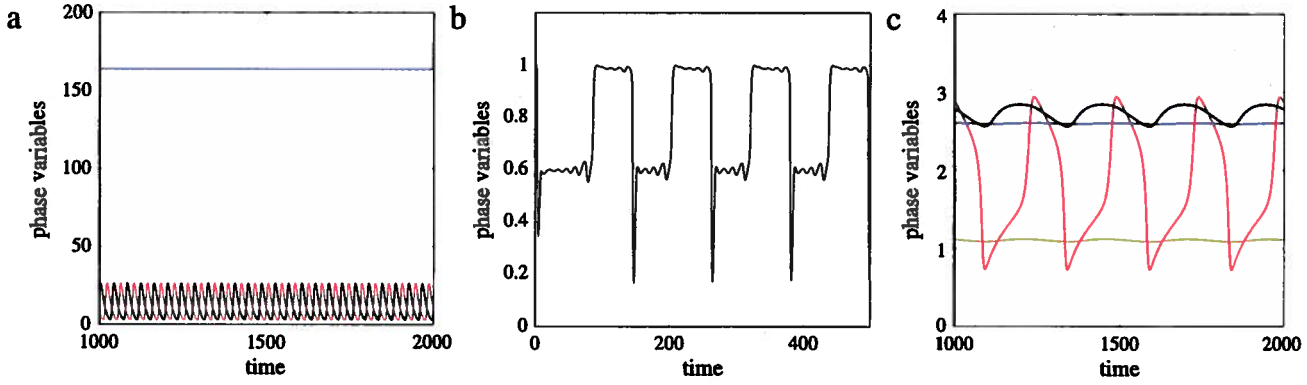

Fig. 14. *OD*-related oscillatory solutions. (a) Inhomogeneous limit cycle is characterized with small oscillations around the two spatially nonuniform centers—the stable *OD* branches (*IHLC* manifestation for the system of coupled repressilators (Eq. (A.3))). (b) Mixed-mode oscillations consist of small-amplitude high-frequency oscillations that alternate with the single large-amplitude long-period cycle (representative example for the system of coupled neurons—Eq. (A.8)). (c) Partial *OD* regime represents a complex oscillatory solution where part of the oscillators populate the upper and lower branches of the *OD*, others perform low amplitude oscillations around these solutions, whereas others run along the full cycle. Within each cluster the oscillators exhibit identical behavior. Demonstration of this solution is given for the system of coupled genetic oscillators (Eq. (7)). Here, a 4-clusters manifestation is shown, with 4 oscillators in each cluster. All solutions are for systems of $N = 16$ coupled oscillators. Different colors denote different stable clusters. (For interpretation of the references to colour in this figure legend, the reader is referred to the web version of this article.)

investigated oscillators. In the membrane model (Section 3.1.1 and [103]) for example, it has been shown that the transition from *IHSS* to anti-phase mixed-mode oscillations is realized via an infinite period bifurcation in the region of strong interactions. In this system, the appearance of the mixed-mode solution can be considered as a result of the interaction between the anti-phase mode and the spatially inhomogeneous limit cycle: the *IHLC* locates around an unstable focus that is an inhomogeneous stationary solution outside the region of stable *IHSS*, and the frequency of small oscillations in the mixed-mode corresponds to the frequency associated with the unstable focus and the *IHLC*. The existence of one-, two- and *n*-looped mixed-mode regimes as *isolas* (closed curve without any evidence of bifurcations to other attractors) that coexist with the neighbors have been shown in this model. In neuronal systems (A.8), on the other hand, the transition between *OD* and mixed-mode oscillations is determined by a singular Hopf bifurcation [42]. Characteristic for this transition is that there is an equilibrium point of the original system in the neighborhood where small oscillations occur. Then the intersection of the stable and unstable manifolds of this equilibrium point, together with those of the stable and unstable slow manifolds, contribute to the generation of the mixed-mode solutions in the vicinity of the *OD*. The classification of mixed-mode oscillations and their relation to *OD* is especially important in neuronal systems, since they have been found to exist in central pattern generators such as the lower brain stem network that generates the respiratory rhythm in mammals [108], or in electrophysiological studies of spiny stellate cells in layer II medial entorhinal cortex [109].

5.3. Partial OD

The importance of *OD* and its interpretation, especially for biological systems, renders it necessary to address also the question of the complexity of dynamical regimes in the vicinity of a non-classical stable *IHSS* solution, as the one described in Section 3.1.1. There, we discussed the fact that local coupling structures can give rise to a large number of stable attractors, among which the novel manifestation of *OD* via multiple stable branches was of particular interest. This solution is in turn directly related to a number of different mixed complex solutions, where some of the oscillators are located in the stable *OD* regimes, whereas others perform oscillatory behavior with various amplitude values [82]. Here, we term these solutions as *partial OD regimes*. In the most simple case of 3 locally coupled genetic relaxation oscillators, the partial *OD* regime is defined as a solution where two of the oscillators populate the two stable branches of *OD* (the upper and the lower one), whereas the third oscillator runs along a full cycle providing low amplitude oscillations of the other two. In the general case, for $N > 3$, the oscillatory solutions around *OD*, and thus the partial *OD* regime are more complex. A representative example of a partial *OD* regime is given in Fig. 14c for $N = 16$ coupled genetic relaxation oscillators. In this manifestation, part of the oscillators populate the upper and lower branches of *OD*, others perform low amplitude oscillations around these solutions, whereas the remaining oscillators run along the full cycle. What is important to note is that the partial *OD* regime can be also found for other models exhibiting stable *IHSS*, i.e. the membrane model (A.2). However, the manifestation of this solution is model-dependent, thus no clear classification of these regimes could be provided.

Generally, the dynamical solutions associated with the *OD* regime, as well as the complex behavior and various *OD* manifestations that can be obtained for an increased size of the systems or different coupling structures point to an inhomogeneous regime enhancement. These solutions have in turn direct implications on the characteristics or functionality of the investigated physical, chemical or biological systems. Moreover, it is also necessary to differentiate these solutions from their counterparts in the *AD* oscillation quenching type (i.e. between partial *OD* and partial *AD* regime, discussed further in Section 6.4), mainly due to their different physiological meaning, for example, in neuronal systems. It is important to state

however, that the characterization of *OD* and *OD*-related regimes contributes to their understanding, which can serve as a basis to establish mechanisms to control the dynamical behavior of natural and man-made systems of coupled oscillators.

6. Characteristics of the AD phenomenon

In contrast to *OD*, amplitude death is manifested with the presence of a homogeneous steady state—for certain coupling strength, the oscillations are entrained and the oscillators populate the same stable steady state of the system. As recently overviewed in [51], several different routes can lead to stabilization of an unstable steady state and manifestation of *AD*: difference between the frequencies of the oscillators, time-delayed interactions, dynamic, nonlinear and velocity coupling, linear augmentation, etc. In what follows, we discuss very briefly the most common mechanisms that lead to *AD*; for a more extensive discussion on *AD* manifestation and control we refer the reader to [51]. Moreover, by characterizing the occurrence of *AD* and *OD* in a single system of coupled neuronal oscillators, we stress once more the difference between these two distinct dynamical regimes, and point out the importance of a proper classification of the oscillation quenching type not only from a viewpoint of dynamical control, but also from application aspects. Additionally, the identification of the differences between the oscillation-quenching-related dynamical regimes, such as partial amplitude and oscillation death support as well the arguments presented here.

6.1. AD via eigenfrequency distribution of the coupled oscillators

One of the early observations that coupling can stabilize the origin of a system of coupled oscillators was made by Yamaguchi and Shimizu [110], who found that two ingredients are needed for *AD* to occur: (i) sufficiently strong coupling and (ii) a critical width of the natural frequency distribution of the coupled oscillators. Further on, it was shown that *AD* is a robust phenomenon persisting for a wide range of systems independent of the spatial symmetries or coupling characteristics, as well as the number of different frequency distributions: the homogeneous steady state, and thus *AD* can be stabilized for a random distribution of frequencies between the coupled oscillators, as well as when the natural frequencies are equally spaced at certain intervals [48,111,41,94,112,113].

In particular, examining a system of coupled Landau–Stuart oscillators under global coupling

$$\frac{dz_i}{dt} = (1 - |z_i|^2 + i\omega_i)z_i + d(\langle z\rangle - z_i) \tag{10}$$

where $\langle z\rangle = \frac{1}{N}\sum_{j=1}^{N} z_j$, it can be shown that the stability of the *AD* solution depends on whether the characteristic equation of system (Eq. (10)) has roots μ_i with $\mathbb{R}e\,\mu_i \leq d - 1 > 0$. Generally, the main conditions for the occurrence of *AD* in systems of coupled oscillators with a random distribution of the natural frequencies can be written as: $d > 1, f(d-1) < d^{-1}$ [50]. This means that for sufficiently strong coupling and frequency dispersion, the oscillators pull each other off their limit cycles into the origin, which is stabilized via an inverse Hopf bifurcation, as we already discussed in Section 2.2.

Moreover, the stabilization of the steady state in this manner was shown experimentally using electrochemical oscillators coupled through an external electronic circuit [114], thus confirming the theoretical predictions that the invariant torus of the coupled system shrinks to zero as the coupling of the system is increased [111]. Similar observations of *AD* have been also discussed for lasers [35,115], as well as theoretical models of oscillatory cardiac pacemaker cells surrounded by passive fibroblast elements [116]. It is interesting to note here once again that introducing random frequency deviations from a regular, smooth trend of the natural frequencies of the coupled oscillators can eliminate *AD* [102], in contrast to the parameter mismatch as introduced in Section 4, which was shown to enhance the dominance of an *OD* regime.

6.2. Time-delayed interactions and occurrence of AD

If the frequencies of the oscillators are identical, then the formation of *AD* can occur if time-delayed interactions of the form

$$\frac{dz_i}{dt} = (1 - |z_i|^2 + i\omega_i)z_i + d(z_j(t-\tau) - z_i) \tag{11}$$

are present in the system [117,118]. Here, τ is a measure of the time delay. In particular, for the coupled Landau–Stuart oscillators in the form given by Eq. (11), the region of intersection between the curves $\tau = \frac{\cos^{-1}(1-1/d)}{\omega-\sqrt{2d-1}}$ and $\tau = \frac{\pi-\cos^{-1}(1-1/d)}{\omega+\sqrt{2d-1}}$ determines the only stability region (of the origin) that takes place as a function of τ [117]. In [117], the authors also discuss *AD* occurrence for an arbitrary number of coupled identical oscillators.

Since a time delay effect arises naturally from the finite propagation time of information signals exchanged between the coupled units, oscillation quenching via time delay has been significantly investigated both theoretically and experimentally. It has been shown, for example, that distributed delays enlarge the *AD* stability regions in the parameter space [119]. Moreover, when the variance in the distribution is larger than a given threshold, the death region is unbounded, and *AD* can occur for $\forall\tau > 0$ [119]. Additionally, detailed theoretical studies for oscillators locally coupled on a ring [120], as well

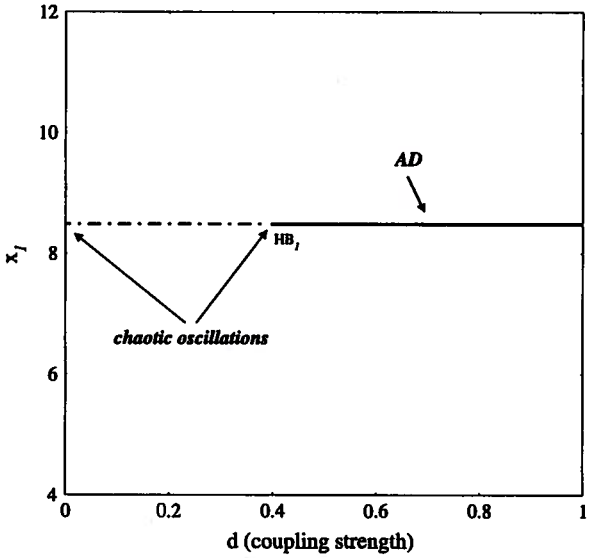

Fig. 15. Manifestation of *AD* for two chaotic Lorenz oscillators coupled via dissimilar variables (System (A.9)). Parameters as in [123].

as experimental manifestations of *AD* for optothermal oscillators located on the same interferometric device and thermally coupled [121] and electronic circuits [122] have been performed.

A large class of interest here are systems of coupled chaotic oscillators and the conditions for *AD* occurrence, since *AD* can be seen as a stabilization criterion and a possibility to control chaotic dynamics [94,95,38]. It is interesting to discuss the route to *AD* in chaotic systems and compare it with previous observations of *OD* in the same systems. In particular, for time-delayed coupled identical chaotic Lorenz oscillators it has been shown that the transition to *AD* occurs directly from chaotic dynamics to a fixed point [38], in contrast to the *OD* case (the details of the chaos $\rightarrow$ *OD* transitions for the Lorenz system are discussed in Section 3.3 and [39]). A similar transition occurs also for chaotic Lorenz oscillators coupled via dissimilar variables [123], where the transition from chaotic dynamics to stable *AD* occurs via a Hopf bifurcation, as shown in Fig. 15. We underline here once more the differences between *AD* and *OD*: in the case of *OD*, the coupled Lorenz oscillators populate the different branches of the stable *IHSS*, whereas when stable *AD* is observed, the coupled Lorenz oscillators go to the same homogeneous steady state.

In general, this transition mechanism, especially for time-delayed systems, implies that even though neither an unstable periodic orbit is stabilized, nor new periodic solutions are created, the time-delayed interaction is a sufficient condition to stabilize the fixed point directly, leading to an abrupt change in the largest Lyapunov exponent of the system, which becomes negative for a given τ, thus determining the onset of *AD*.

However, it has been also shown that the stability region of *AD* in systems of N delay-coupled oscillators can be reduced if a specific, i.e. gradient coupling is used [124]. Consider for example the situation when Landau–Stuart oscillators are coupled with an anisotropic time-delay coupling with their neighbors in the form

$$\frac{dz_i}{dt} = (1 - |z_i|^2 + i\omega_i)z_i + (d + r)(z_{i+1}(t - \tau) - z_i) + (d - r)(z_{i-1}(t - \tau) - z_i) \tag{12}$$

where r here is the gradient coupling strength and τ, as before, denotes the delay in the interaction. An increasing strength of the gradient coupling monotonically reduces the domain of the death islands in the (d, τ) parameter space, and thus the *AD* stability islands can be completely eliminated once the gradient coupling r exceeds a critical threshold. The value of this threshold was found to be constant if the number of coupled oscillators N is sufficiently large [124].

Thus, the importance of *AD* has been noted by many authors in relation to various, physical, chemical or biological phenomena, since many natural or man-made systems can be studied as systems of coupled oscillators. It has been verified that *AD* is a general phenomenon, realized for periodic, chaotic, hypercaotic and time delayed systems and also for various coupling types, i.e. diffusive, replacement, conjugate coupling, coupling via scalar signals, nonlinear and velocity coupling, etc. ([125,53,126] and others).

This clearly shows that both oscillation quenching types, *AD* and *OD* are important regulators of a system's dynamics and can be used as stabilization routes in a wide range of systems. However, we emphasize here once more the fact that *AD* and *OD* refer to two structurally distinct dynamical regimes, homogeneous and inhomogeneous steady states. Thus, classifying this difference is significantly important, especially for biological systems, since it leads to diverse meaning and interpretation of the dynamical state of the system. We therefore analyze next a system of coupled neuronal oscillators, stressing once more the necessity to distinguish between both oscillation quenching types discussed in the work.

6.3. Transition between AD and OD in neuronal systems and physiological implications

Firing rate models of neuronal oscillators have been extensively studied in the literature, as a means to understand various dynamical behavior, such as neural competition, central pattern generators, frequency control in neuronal networks, etc. This is important because various dynamical regimes have been directly related to certain pathological cases, i.e. it has been speculated that the essential tremor that occurs in Alzheimer's or Parkinson's disease is a direct consequence of synchronous firing of neuronal populations [27,29,28], whereas *OD* has been implied as a background mechanism for selection and switching in the basal ganglia under normal and pathological conditions [99,100]. Under such conditions, the oscillation quenching type plays a crucial role, since it can lead either to a stabilization phenomenon, i.e. *AD* in the case of Parkinson's disease, or a different pathological situation (*OD*-related effects in the basal ganglia). Therefore, by studying next a model of coupled neuronal oscillators, the Wilson–Cowan system, we emphasize once more the structural difference between *AD* and *OD*, underlying the fact that both oscillation quenching types can occur in a single neuronal population and can lead to a different dynamical behavior with different physiological meaning, as already stated.

Generally, the Wilson–Cowan model (Eq. (A.10)) describes the interactions between an excitatory and inhibitory population of neurons [49]. For simplicity, we treat here one such network as a single oscillator. In this case, the system is characterized with a non-diffusive, synaptic coupling, displaying a stable limit cycle behavior for a wide parameter range. Additionally, quenching of oscillations in the form of *AD* can be also observed when only excitatory–excitatory (β_{ee}) coupling between the neurons is present (Fig. 16a and [49]).

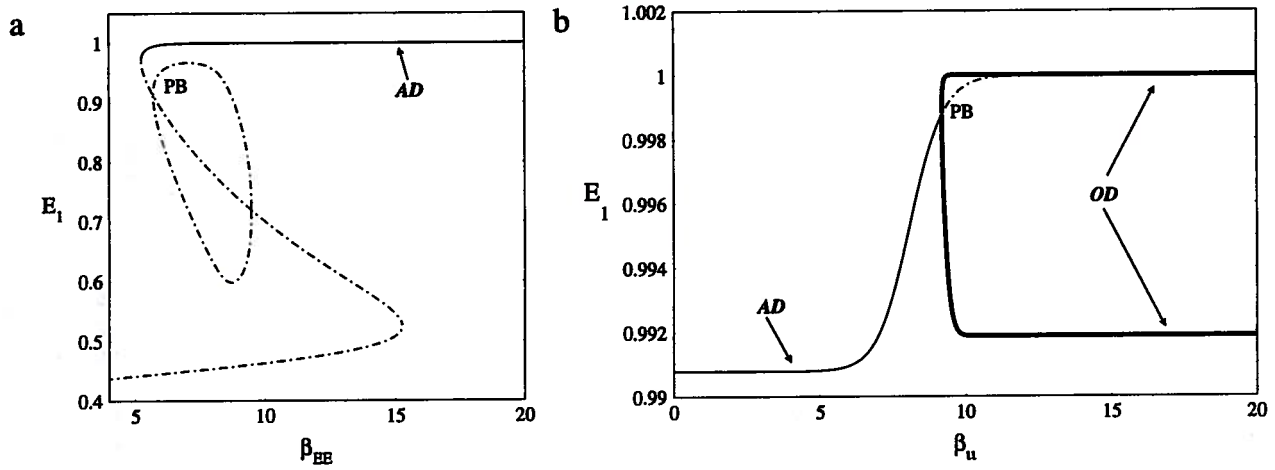

Fig. 16. Amplitude and oscillation death in the Wilson–Cowan model of interacting neuronal populations. (a) *AD* is observed for excitatory–excitatory (β_{ee}) coupling, (b) whereas presence of additional inhibitory–inhibitory (β_{ii}) coupling leads also to stabilization of *OD*. The transition $AD \rightarrow OD$ is of Turing type.

In this case, the formation of *AD* is significantly different than the routes to *AD* previously described (a difference in the frequencies or time-delay in the interactions). *AD* here appears due to the lack of uniformity of the local frequency along the limit cycle of the coupled system. An important characteristic of this mechanism is that the coupling does not vanish identically when the oscillators (or the neuronal populations) are in the same phase. Thus, the oscillations are quenched and the homogeneous steady state is stabilized via an infinite period bifurcation ($\beta_{ee} \sim 5.3$ in Fig. 16a). This means that *AD* can be used to stabilize neuronal oscillations, and therefore represents a possible control mechanism. However, what is important to stress here is that the systems display as well an inhomogeneous steady state, or *OD*, which is unstable under these conditions (the reason for *OD* appearance is the symmetry breaking of the *HSS* via a *PB*, as discussed in Section 3 and shown in Fig. 16a. We note that the possibility for *OD* has not been identified in [49]). Introducing additionally an inhibitory–inhibitory coupling in the system allows for a supercritical pitchfork bifurcation to occur, resulting in a stable *OD* solution (Fig. 16b). Moreover, a transition from *AD* to *OD* characterized with a Turing-type bifurcation (as discussed in Section 2.3) is again observed. Physiologically speaking, a transition from a dynamical state where a certain pathological condition of firing neurons has been stabilized (*AD*), to a "winner-take-all" regime (*OD*) could be possibly related to the occurrence of novel pathological conditions in the basal ganglia, as previously suggested [100]. However, the implications of the transition between both oscillation quenching types in neuronal populations awaits physiological interpretations. Nevertheless, the example presented here underlines two very important facts: (i) *AD* and *OD* are two structurally distinct dynamical regimes, which is in turn directly related to the interpretation and control of the (physiological) observations and (ii) the transition scenario between both oscillation quenching types persists to exist under various conditions (different mechanism of *AD* occurrence and different coupling types).

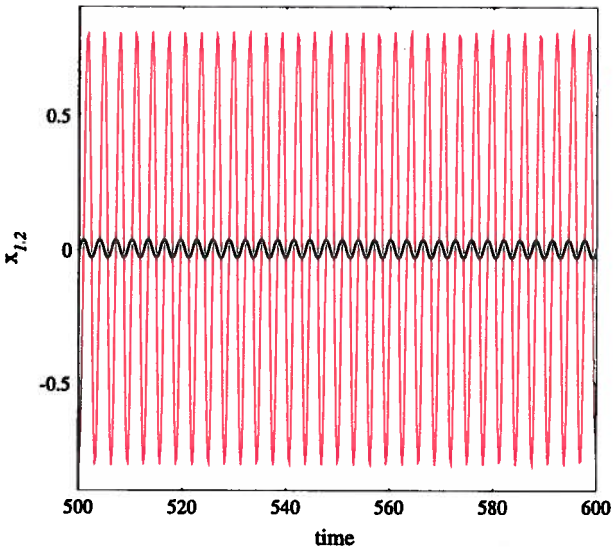

Fig. 17. Manifestation of *AD* for two nonidentical Landau–Stuart oscillators ($\Delta = 5$), diffusively coupled via both variables. One of the oscillators performs small-amplitude oscillation around the origin, whereas the second one exhibits high-amplitude oscillations.

6.4. Partial amplitude death

Similarly to *OD*, *AD* is also accompanied (in parameter space) by an additional dynamical regime, the *partial amplitude death*. Partial *AD* is defined as a dynamical solution where a part of the coupled oscillators is almost quenched, whereas the others remain to oscillate [60] (manifestation of partial *AD* for a system of coupled Landau–Stuart oscillators is given in Fig. 17). Even though this definition of partial *AD*, and thus its manifestation resembles the characteristics of partial *OD* which we previously discussed (Section 5.3 and Fig. 13c), these two regimes are significantly different. Generally, partial *AD* occurs when the individual coupled units are *significantly different* (in amplitude and phase) [127]. For example, the authors in [102] considered a special case where the natural frequencies of the oscillators are distributed in a regular monotonic trend and determined the limiting frequency mismatch for which partial *AD* can be observed. Moreover, they also showed that partial amplitude death is weakened by introducing random deviations from the linear trend of frequencies.

Generally speaking, in a certain interval of the coupling strength, a manifestation of partial *AD* follows this particular scenario: some of the coupled oscillators are damped (the amplitude is not exactly zero, thus they perform small amplitude oscillations around the homogeneous origin of the system which remains unstable), whereas the rest of the population continues to exhibit high-amplitude oscillations (see Fig. 17). In this case, the damped oscillators go to the same homogeneous steady state of the system, which distinguishes this regime from the partial *OD* solution: when partial *OD* is observed, part of the oscillators exhibit damped oscillations in the vicinity of the *two* stable *OD* branches of the *IHSS* (Fig. 13c), which are spatially separated, whereas the remaining oscillators, similarly to the partial *AD* case, perform high amplitude oscillations. Importantly, a significant difference is also underlined by the fact that partial *OD* occurs for *identical* units. We emphasize here that the difference in partial *AD* and *OD* regimes is a direct consequence of the structural difference and the distinction in the generation mechanisms of both oscillation quenching types, *AD* and *OD*.

Moreover, partial *AD* has been proposed as a "transition solution" which occurs during the road to complete *AD*, where all of the oscillators are suppressed and go to the homogeneous steady state of the system [125]. Additionally, partial *AD* has been also observed for coupled chaotic oscillators [128]. In terms of the studied networks, partial *AD* can be related to the formation of spatial patterns consisting of oscillating and suppressed units.

7. Summary

Oscillation quenching in the form of *AD* and *OD*, as well as the characterization of their mechanisms of occurrence, has attracted considerable attention in the past decades due to the generality of these phenomena and their broad application purposes. Even though the mathematical classification clearly separates them as distinct dynamical regimes, very often *AD* and *OD* have been used in the literature without a strong discrimination. Therefore, this review aimed at highlighting the specificities of the inhomogeneous (*OD*) and homogeneous steady states (*AD*), as a means to set clear definition boundaries between both oscillation quenching types.

The main part was here devoted to the *OD* phenomenon, as it is significantly less studied than *AD*. The generality of the symmetry breaking scenario which leads to a formation of an *IHSS* via a pitchfork bifurcation of the steady state in the presence of stable coupled limit cycles, was demonstrated for systems that differ in their dynamical structure and coupling organization. This characteristic bifurcation scenario further opens the possibility for coexistence of *OD* and oscillations, both periodic and chaotic, as a typical solution for systems exhibiting an *IHSS*. Moreover, the principle of *OD* generation

underlines additionally its clear difference with *AD*, which generally emerges via a Hopf or a saddle–node bifurcation from a limit cycle to a homogeneous steady state, through which it is manifested. The different generation, and consequently manifestation scenarios of *OD* and *AD* distinguish further their application purposes: oscillation quenching can induce either stabilization (*AD*) or variability (*OD*) in a given oscillatory system. Thus, the role of *OD*, manifested as two stable branches on the *IHSS*, especially for biological (biochemical) systems was extensively discussed. *OD* can be directly related to basic biochemical phenomena, such as cellular differentiation [55,56], pattern formation [66], dynamical behavior of neuronal populations [42], etc. Here, it is necessary to stress the importance of *OD* for technical systems as well: thermo-kinetic oscillators, for which *OD* manifestation has been experimentally shown, are of direct relevance to industrial processes [35]. In these cases, *OD* can play a vital role in the safety measures. In contrast to this, *AD* can be understood in terms of stabilizing a specific homogeneous steady state by different means, mainly frequency difference or time-delayed interactions. This question is of significant importance for technical systems, i.e. laser or chaotic systems, as well as natural, e.g. neuronal networks and certain pathological conditions that occur.

On the other hand, the interaction between *OD* and small parameter mismatches can be seen as an amplifier of the variability that is produced by this oscillation quenching mechanism. This interplay allows *OD* to dominate in parameter space, removing completely the coexisting oscillatory solutions. Thus, the *ODD* effect, which was shown to be model-independent, provides an efficient regulator that can be used for technological purposes.

Additional to the classical *OD* manifestation, and the fact that it provides heterogeneity in a stable homogeneous medium, partial *OD* strongly extends the variability of the observed limit cycle solutions. Even though partial *OD* in the case of identical oscillators was found to be model-specific, the richness of the exhibited dynamical solutions, even in the case of coupled identical oscillators is notable. Examples are asymmetric oscillations characterized with a large difference in the amplitude between the oscillators, or the so-called "dynamic-trap" solution [129], where the oscillators placed at a largest distance oscillate in anti-phase, where the middle one(s) perform small amplitude oscillations. All these solutions extend the dynamical structures which can occur around the stability region of *OD*, and can be further exploited for application purposes. Moreover, we can expect that for small parameter mismatches, similarly to the *ODD* example, partial *OD* is model independent and occupies larger areas in parameter space.

The fact that it is possible to observe both *AD* and *OD* in a single system highlights further the necessity for proper distinction between both regimes, since they lead to different dynamical behavior, further resulting in diverse meanings and interpretations. This is significantly pronounced when studying neuronal networks for example, where a large amount of work, especially on the physiological interpretation still lies ahead.

Throughout this review we tried to summarize the current knowledge for the characterization of both oscillation quenching phenomena, *OD* and *AD*, pointing not only to their theoretical significance, but also possibilities for their application as control mechanisms. It is however, important to note here that effects, inverse of *OD* and *AD* have been postulated in the literature. For example, in 1974 S. Smale discussed the possibility to "produce oscillations due to linear coupling of two different kind of processes, each processes in itself stationary" [130]. This idea has been regarded as a mechanism inverse to *OD* and *AD*, since, as shown in this review, quenching of oscillations occurs due to the coupling present in the systems. Thus, Smale's effect can be considered as a motivation for new investigations in this direction.

Acknowledgments

AK acknowledges the Frauenförderungsprogramm der Humboldt-Universität Berlin, EV the RFBR 12-02-00529a and JK the IRTG 1740 (DFG, FAPESP) and SUMO (EU).

Appendix A. Mathematical models

Here we list the mathematical models used in the examples of this paper:

- Morris–Lecar-like β-cell model [131,65]

$$\begin{aligned}\frac{dV_i}{dt} &= \frac{1}{C_m}(I_{app} - I_{i_K} - I_{i_{K(ATP)}} - I_{i_{C_a}} - I_{i_{K(C_a)}} - I_{i_c})\\ \frac{c_i}{dt} &= f_{cyt}(-\alpha I_{i_{C_a}}(V_i) - k_{PMCA}c_i + g_{c,C_a}(c_j - c_i))\end{aligned} \tag{A.1}$$

where V_i represents the membrane potential, and c_i accounts for the cytosolic calcium concentration, $[Ca^{2+}]_i$ in the i-th oscillator. The parameter $k^{(i)}_{PMCA}$ denotes the plasma membrane $C_a^{2+}ATP$ ase pump rate, and is used as a bifurcation parameter here. Other variables have the same notation and values as in Ref. [65].

- The membrane model [83,69]

$$\begin{aligned}\frac{dx_i}{dt} &= \frac{1}{\varepsilon}\left(k + 0.5x_iy_i - x_i^2 - \frac{1.5\gamma x_i}{x_i + \delta}\right)\\ \frac{dy_i}{dt} &= \eta^{(i)} - 1.5x_iy_i - Dy_i - \frac{0.5\gamma x_i}{x_i + \delta} + d(y_{i+1} - y_i).\end{aligned} \tag{A.2}$$

The parameter ε controls the stiffness of the oscillators and could vary between 0.1 and 0.01, and d denotes the coupling strength. k, γ, D, δ and η are the rates of influx and efflux of participants. The first four are kept fixed ($k = 0.05, \gamma = 0.5$, $D = 0.2, \delta = 0.15$) and η is considered as a bifurcation parameter. These equations are derived from a realistic set of chemical equations, but for our purposes here, we will omit all physico-chemical details and consider this system as a paradigmatic model for an oscillator of relaxation type.

- Repressilator model:

$$\begin{aligned}
\dot{a}_i &= -a_i + \frac{\alpha}{1 + C_i^n} \\
\dot{b}_i &= -b_i + \frac{\alpha}{1 + A_i^n} \\
\dot{c}_i &= -c_i + \frac{\alpha}{1 + B_i^n} + \kappa \frac{S_i}{1 + S_i} \\
\dot{A}_i &= \beta_a (a_i - A_i) \\
\dot{B}_i &= \beta_b (b_i - B_i) \\
\dot{C}_i &= \beta_c (c_i - C_i) \\
\dot{S}_i &= -k_{s0} S_i + k_{s1} B_i - \eta (S_i - S_e)
\end{aligned} \tag{A.3}$$

where $S_e = Q\bar{S}$, and $\bar{S} = \frac{1}{N}\sum_{i=1}^{N} S_i$. $a_i(A_i)$, $b_i(B_i)$ and $c_i(C_i)$ represent the concentrations of mRNA(protein) molecules transcribed from the genes of *tetR*, *cI* and *lacI*, respectively, and S_i denotes the concentration of *AI* molecules. Q is the coupling coefficient and will be used as a bifurcation parameter. The parameters are defined as in [86].

- Model of coupled Brusselators:

  In [47], Prigogine and Lefever considered the model:

$$\begin{aligned}
\frac{dx_i}{dt} &= A^{(i)} - (B + 1)x_i + x_i^2 y_i + d_x(x_j - x_i) \\
\frac{dy_i}{dt} &= Bx_i - x_i^2 y_i + d_y(y_j - y_i)
\end{aligned} \tag{A.4}$$

where A and B are the system's parameters, and d_x and d_y are coupling coefficients. The system possesses a single homogeneous steady state for

$$x_i = A, \qquad y_i = B/A, \quad i = 1, 2$$

which becomes unstable when

$$B = B_c = (1/2d_y)(A^2 + 2d_x A^2 + 2d_y + 4d_x d_y)$$

determining that instability occurs only for a finite range of values of the diffusion coefficients. Thus, for (i) $B \leq B_c$ only the homogeneous steady state solution is stable. All other solutions do not have physical meaning, and are therefore not considered; (ii) for $B > B_c$ there exist two solutions: one is the continuation of the *HSS* and the other is the *IHSS*. The stability boundaries of the *IHSS* depend on the parameter values. The inhomogeneous solution is double degenerate, since the indices 1 and 2 are interchangeable. Thus, the two oscillators, although identical, will not have the same values of the phase variables, which corresponds to the definition of *OD*: two stable branches of the *IHSS* which are separated in space.

- Oregonator model:

$$\begin{aligned}
\frac{dx_i}{dt} &= \frac{1}{\varepsilon}\left(x_i(1 - x_i) - fz_i \frac{(x_i - q)}{q + x_i}\right) \\
\frac{dz_i}{dt} &= x_i - z_i + d(z_j - z_i)
\end{aligned} \tag{A.5}$$

where ε, q and f are kinetic parameters related to the reagent reaction rates, x and z are proportional to the concentration of $HBrO_2$ and metal ions, and d is the coupling coefficient [8].

- Chaotic oscillators: Lorenz system

$$\begin{aligned}
\frac{dx_i}{dt} &= \sigma(y_i - x_i) \\
\frac{dy_i}{dt} &= rx_i - y_i - x_i z_i \\
\frac{dz_i}{dt} &= x_i y_i - bz_i + d(x_j - x_i).
\end{aligned} \tag{A.6}$$

The non-symmetrical equilibria of the system are characterized with $A_{1/2} = (x_1^*, x_1^*, r-1, x_2^*, x_2^*, r-1)$, (i) where $x_2^* = 2d - x_1^*$, and $x_1^* = d + \sqrt{b(r-1) - d^2}$ for A_1 and (ii) $x_1^* = d - \sqrt{b(r-1) - d^2}$ for A_2; and $A_{3/4} = (0, 0, \frac{dx_2^*}{b}, x_2^*, x_2^*, r-1)$ with $x_2^* = (d + \sqrt{a^2 + 4b(r-1)})/2$ for A_3. The values of $A_{1/2}$ and A_3 are represented in Fig. 11a. Here, $\sigma = 10, r = 28$ and $b = \frac{8}{3}$.

- Coupled Pikovsky–Rabinovich (*PR*) circuits:

$$\begin{aligned} \frac{dx_i}{dt} &= y_i(t) - \beta z_i(t) \\ \frac{dy_i}{dt} &= -x_i(t) + 2\gamma y_i(t) + \alpha z_i(t) + d(y_j(t) - y_i(t)) \\ \frac{dz_i}{dt} &= (x_i(t) - z_i(t)^3 + z_i(t))/\mu \end{aligned} \tag{A.7}$$

where α, β, γ and μ are system's parameters ($\alpha = 0.165, \beta = 1, \gamma = 0.26, \mu = 0.4$) and d is the coupling strength. The origin of the uncoupled *PR* circuit is an unstable steady state.

- Two-cell inhibitory neural network with adaptation

$$\begin{aligned} \frac{du_1}{dt} &= -u_1 + S(I - \beta u_2 - g a_1) \\ \frac{du_2}{dt} &= -u_2 + S(I - \beta u_1 - g a_2) \\ \varepsilon \frac{da_1}{dt} &= -a_1 + u_1 \\ \varepsilon \frac{da_2}{dt} &= -a_2 + u_2 \end{aligned} \tag{A.8}$$

where $\varepsilon \gg 1$ and S is a nonlinear gain function that satisfies the following conditions: (i) S is differentiable, (ii) is monotonically increasing from $\lim_{x\to-\infty} S(x) = 0$ to $\lim_{x\to\infty} S(x) = 1$ and with (iii) convexity-change at $x = \vartheta$. S is a sigmoidal function and it depends on two parameters (positive r and real ϑ) that control its slope and activation threshold: $S(x) = \frac{1}{1+\exp^{-r(x-\vartheta)}}$. Competition in the model is achieved through mutual inhibition of the neurons of strength β and a negative feedback (such as spike frequency adaptation) of strength g. Additionally, each cell has an external stimulation of equal strength I. The parameters are chosen from [42].

- Lorentz oscillators coupled via dissimilar variables

$$\begin{aligned} \frac{dx_i}{dt} &= \sigma(y_i - x_i) \\ \frac{dy_i}{dt} &= r x_i - y_i - x_i z_i + d(y_j - x_i) \\ \frac{dz_i}{dt} &= x_i y_i - b z_i \end{aligned} \tag{A.9}$$

with $\sigma = 10, r = 28$ and $b = \frac{8}{3}$.

- Wilson–Cowan model of coupled neuronal oscillators

$$\begin{aligned} \frac{dE_j}{dt} &= -E_j + S(\alpha_{ee} E_j - \alpha_{ie} I_j + \beta_{ee} E_k - \beta_{ie} I_k - \nu_e) \\ \frac{dI_j}{dt} &= -I_j + S(\alpha_{ei} E_j - \alpha_{ii} I_j + \beta_{ei} E_k - \beta_{ii} I_k - \nu_i) \end{aligned} \tag{A.10}$$

where $E(t)$ and $I(t)$ determine the respective firing rates of the excitatory and inhibitory neurons (neuronal populations). The parameters $\alpha_{ee}, \alpha_{ie}, \alpha_{ei}$ and α_{ii} determine the synaptic strength between both neuronal populations, ν_e and ν_i are the respective threshold for firing, whereas $\beta_{ee;ie;ei;ii}$ represent the coupling between the two populations. For example, β_{ie} is the coupling between the inhibitory cells from population j to excitatory cells from population k and so on. S is here a piecewise-linear function defined as $S(u) = .5(1 + \tanh(u))$.

References

[1] P. Hadley, M.R. Beasley, K. Wiesenfeld, Phase locking of Josephson-junction serries arrays, Phys. Rev. B 38 (1988) 8712–8719.
[2] P. Hadley, M.R. Beasley, K. Wiesenfeld, Phase locking of Josephson-junction arrays, Appl. Phys. Lett. 52 (1988) 1619–1621.
[3] P.M. Varangis, A. Gavrielidis, T. Erneux, V. Kovanis, L.F. Lester, Frequency entrainment in optically injected semiconductor lasers, Phys. Rev. Lett. 78 (1997) 2353–2356.

[4] A. Hohl, A. Gavrielidis, T. Erneux, V. Kovanis, Localized synchronization in two coupled nonidentical semiconductor lasers, Phys. Rev. Lett. 78 (1997) 4745–4748.
[5] J. Benford, H. Sze, W. Woo, R.R. Smith, B. Harteneck, Phase locking of relativistic magnetrons, Phys. Rev. Lett. 62 (1989) 969–971.
[6] I. Schreiber, M. Marek, Strange attractors in coupled reaction–diffusion cells, Physica D 5 (1982) 258–272.
[7] Y. Kuramoto, Chemical Oscillations, Waves and Turbulence, Springer, Berlin, 1982.
[8] M.F. Crowley, I.R. Epstein, Experimental and theoretical studies of a coupled chemical oscillator: phase death, multistability, and in-phase and out-of-phase entrainment, J. Phys. Chem. 93 (1989) 2496–2502.
[9] M. Dolnik, I.R. Epstein, Coupled chaotic chemical oscillators, Phys. Rev. E 54 (1996) 3361–3368.
[10] S. Daan, C. Berde, Two coupled oscillators: simulations of the circadian pacemaker in mammalian activity rhythms, J. Theoret. Biol. 70 (1978) 297–314.
[11] M. Kawato, R. Suzuki, Two coupled neural oscillators as a model for the circadian pacemaker, J. Theoret. Biol. 86 (1980) 547–575.
[12] D. Golomb, D. Hansel, G. Mato, Mechanisms of synchrony of neural activity in large networks, in: Handbook of Biological Physics, Elsevier, Amsterdam, 2001.
[13] C. Li, L. Chen, K. Aihara, Transient resetting: a novel mechanism for synchrony and its biological examples, PLoS Comput. Biol. 2 (2006) e103.
[14] P. Menck, J. Kurths, Topological identification of weak points in power grids, in: Proceedings of the NDES 2012 Berlin: VDE, 2012, pp. 144–147.
[15] A.T. Winfree, The Geometry of Biological Time, Springer, New York, 1980.
[16] J.D. Murray, Mathematical Biology, Springer, New York, Berlin, Heidelberg, 1993.
[17] A. Pikovsky, M. Rosenblum, J. Kurths, Synchronization: A Universal Concept in Nonlinear Sciences, Cambridge University Press, 2001.
[18] S. Boccaletti, J. Kurths, G. Osipov, D. Valladares, C. Zhou, The synchronization of chaotic systems, Phys. Rep. 366 (2002) 1–101.
[19] A. Arenas, A. Diaz-Guilera, J. Kurths, Y. Moreno, C. Zhou, Synchronization in complex networks, Phys. Rep. 469 (2008) 93–153.
[20] R. Roy, S. Thornburg, Experimental synchronization of chaotic lasers, Phys. Rev. Lett. 72 (1994) 2009–2012.
[21] D.K. Welsh, D. Logothetis, M. Meister, S. Reppert, Individual neurons dissociated from rat suprachiasmatic nucleus express independently phased circadian firing rhythms, Neuron 14 (1995) 697–706.
[22] R.Y. Moore, Circadian rhythms: basic neurobiology and clinical applications, Annu. Rev. Med. 48 (1997) 253–266.
[23] S. Yamaguchi, H. Isejima, T. Matsuo, R. Okura, K. Yagita, M. Kobayashi, H. Okamura, Synchronization of cellular clocks in the suprachiasmatic nucleus, Science 302 (2003) 1408–1412.
[24] D. Gonze, S. Bernard, C. Waltermann, A. Kramer, H. Herzel, Spontaneous synchronization of coupled circadian oscillators, Biophys. J. 89 (2005) 120–129.
[25] A. Goldbeter, O. Pouriquié, Modeling the segmentation clock as a network of coupled oscillations in a notch, Wnt and FGF signaling pathways, J. Theoret. Biol. 252 (2008) 574–585.
[26] P. Tass, M. Rosenblum, J. Weule, J. Kurths, A. Pikovsky, J. Volkmann, A. Schnitzler, H.-J. Freund, Detection of n:m phase locking from noisy data: application to magnetoencephalography, Phys. Rev. Lett. 81 (1998) 3291–3294.
[27] P.A. Tass, Phase Resetting in Medicine and Biology. Stochastic Modelling and Data Analysis, Springer, Berlin, 1999.
[28] J. Milton, P. Jung, Epilepsy as a Dynamic Disease, Springer, Berlin, 2003.
[29] G. Buzsaki, A. Draguhn, Neuronal oscillations in cortical networks, Science 304 (2004) 1926–1929.
[30] H. Bergman, A. Feingold, A. Nini, A. Raz, H. Slovin, M. Abeles, E. Vaadia, Physiological aspects of information processing in the basal ganglia of normal and parkinsonian primates, Trends Neurosci. 21 (1998) 32–38.
[31] J. Sarnthein, A. Morel, A. von Stein, D. Jeanmonod, Thalamic theta field potentials and EEG: high thalamocortical coherence in patients with neurogenic pain, epilepsy and movement disorders, Thalamus & Related Systems 2 (2003) 231–238.
[32] M.Y. Kim, R. Roy, J.L. Aron, T.W. Carr, I.B. Schwartz, Scaling behavior of laser population dynamics with time-delayed coupling: theory and experiment, Phys. Rev. Lett. 94 (2005) 088101.
[33] P. Kumar, A. Prasad, R. Gosh, Stable phase-locking of an external-cavity diode laser subjected to external optical injection, J. Phys. B 41 (2008) 135402.
[34] B. Gallego, P. Cessi, Dynamical variability of two oceans and an atmosphere, J. Clim. 14 (2001) 2815–2832.
[35] B.F. Kuntsevich, A.N. Pisarchik, Synchronization effects in a dual-wavelength class-B laser with modulated losses, Phys. Rev. E 64 (2001) 046221.
[36] D. Ruwisch, M. Bode, D. Volkov, E. Volkov, Collective modes of three coupled relaxation oscillators: the influence of detuning, Internat. J. Bifur. Chaos 9 (1999) 1969–1981.
[37] M. Heinrich, T. Dahms, V. Flunkert, S.W. Teitsworth, E. Schöll, Symmetry-breaking transitions in networks of nonlinear circuit elements, New J. Phys. 12 (2010) 113030.
[38] A. Prasad, Amplitude death in coupled chaotic oscillators, Phys. Rev. E 72 (2005) 056204.
[39] W. Liu, E. Volkov, J. Xiao, W. Zou, M. Zhang, J. Yang, Inhomogeneous stationary and oscillatory regimes in coupled chaotic oscillators, Chaos 22 (2012) 033144.
[40] M. Dolnik, M. Marek, Extinction of oscillations in forced and coupled reaction cells, J. Phys. Chem. 92 (1988) 2452–2455.
[41] G.B. Ermentrout, Oscillator death in populations of all to all coupled nonlinear oscillators, Physica D 41 (1990) 219–231.
[42] R. Curtu, Singular Hopf bifurcations and mixed-mode oscillations in a two-cell inhibitory neural network, Physica D 239 (2010) 504–514.
[43] A. Kuznetsov, M. Kaern, N. Kopell, Synchrony in a population of hysteresis-based genetic oscillators, SIAM J. Appl. Math. 65 (2005) 392–426.
[44] A. Koseska, E. Volkov, A. Zaikin, J. Kurths, Inherent multistability in arrays of autoinducer coupled genetic oscillators, Phys. Rev. E 75 (2007) 031916.
[45] J.J. Suarez-Vargas, J.A. Gonzalez, A. Stefanovska, P.V.E. McClintock, Diverse routes to oscillation death in a coupled-oscillator system, Europhys. Lett. 85 (2009) 38008.
[46] A. Turing, The chemical basis of morphogenesis, Philos. Trans. R. Soc. Lond. 237 (1952) 37–72.
[47] I. Prigogine, R. Lefever, Symmetry breaking instabilities in dissipative systems, J. Chem. Phys. 48 (1968) 1695–1700.
[48] D. Aronson, E. Doedel, H. Othmer, An analytical and numerical study of the bifurcations in a system of linearly coupled oscillators, Physica D 25 (1987) 20–104.
[49] G.B. Ermentrout, N. Kopell, Oscillator death in systems of coupled neural oscillators, SIAM J. Appl. Math. 50 (1990) 125–146.
[50] R.E. Mirollo, S.H. Strogatz, Amplitude death in an array of limit-cycle oscillators, J. Stat. Phys. 60 (1990) 245–262.
[51] G. Saxena, A. Prasad, R. Ramaswamy, Amplitude death: the emergence of stationarity in coupled nonlinear systems, Phys. Rep. 521 (2012) 205–228.
[52] K.P. Zeyer, M. Mangold, E.D. Gilles, Experimentally coupled thermokinetic oscillators: phase death and rhythmogenesis, J. Phys. Chem. 105 (2001) 7216–7224.
[53] Y. Zhu, X. Qian, J. Yang, A study of phase death states in a coupled system with stable equilibria, Eur. Phys. Lett. 82 (2008) 4001.
[54] R. Curtu, A. Shpiro, N. Rubin, J. Rinzel, Mechanisms for frequency control in neuronal competition models, SIAM J. Appl. Dyn. Syst. 9 (2008) 609–649.
[55] A. Koseska, E. Ullner, E. Volkov, J. Kurths, J. García-Ojalvo, Cooperative differentiation through clustering in multicellular populations, J. Theoret. Biol. 263 (2010) 189–202.
[56] N. Suzuki, C. Furusawa, K. Kaneko, Oscillatory protein expression dynamics endows stem cell with robust differentiation potential, PLoS One 6 (2011) e27232.
[57] A. Koseska, E. Volkov, J. Kurths, Detuning-dependent dominance of oscillation death in globally coupled synthetic genetic oscillators, Europhys. Lett. 85 (2009) 28002.
[58] A. Koseska, E. Volkov, J. Kurths, Parameter mismatches and oscillation death in coupled oscillators, Chaos 20 (2010) 023132.
[59] E. Ullner, A. Zaikin, E.I. Volkov, J. García-Ojalvo, Multistability and clustering in a population of synthetic genetic oscillators via phase-repulsive cell-to-cell communication, Phys. Rev. Lett. 99 (2007) 148103.
[60] F.M. Atay, Total and partial amplitude death in networks of diffusively coupled oscillators, Physica D 183 (2003) 1–18.
[61] A. Koseska, E. Volkov, J. Kurths, Transition from amplitude to oscillation death via Turing bifurcation, Phys. Rev. Lett. 111 (2013) 024103.
[62] Y. Kuznetsov, Elements of Applied Bifurcation Theory, Springer Verlag, Berlin, 1998.
[63] B. Ermentrout, Simulating, Analyzing, and Animating Dynamical Systems: A Guide to Xppaut for Researchers and Students (Software, Environments, Tools), SIAM Press, 2002.

[64] K. Bar-Eli, On the stability of coupled chemical oscillators, Physica D 14 (1985) 242–252.
[65] K. Tsaneva-Atanasova, C.L. Zimliki, R. Bertram, A. Sherman, Diffusion of calcium and metabolites in pancreatic islets: killing oscillations with a pitchfork, Biophys. J. 90 (2006) 1–13.
[66] M. Toiya, V. Vanag, I. Epstein, Diffusively coupled chemical oscillators in a microfluidic assembly, Angew. Chem., Int. Ed. 47 (2008) 7753–7755.
[67] E. Volkov, V.A. Romanov, Bifurcations in the system of two identical diffusively coupled Brusselators, Phys. Scr. 51 (1995) 19–28.
[68] M.B. Elowitz, S. Leibler, A synthetic oscillatory network of transcriptional regulators, Nature 403 (2000) 335–338.
[69] E.I. Volkov, M.N. Stolyarov, Birhythmicity in a system of two coupled identical oscillators, Phys. Lett. A 159 (1991) 61–66.
[70] D. McMillen, N. Kopell, J. Hasty, J.J. Collins, Synchronizing genetic relaxation oscillators by intercell signaling, Proc. Natl. Acad. Sci. USA 99 (2002) 679–684.
[71] J. García-Ojalvo, M.B. Elowitz, S. Strogatz, Modeling a synthetic multicellular clock: repressilators coupled by quorum sensing, Proc. Natl. Acad. Sci. USA 101 (2004) 10955–10960.
[72] R. Wang, L. Chen, Synchronizing genetic oscillators by signalling molecules, J Biol. Rhyth. 20 (2005) 257–269.
[73] M.R. Atkinson, M.A. Savageau, J.T. Myers, A.J. Ninfa, Development of genetic circuitry exhibiting toggle switch or oscillatory behavior in *Escherichia coli*, Cell 113 (2003) 597–607.
[74] T. Danino, O. Mondragon-Palomino, L. Tsmiring, J. Hasty, A synchronized quorum of genetic clocks, Nature 463 (2010) 326–330.
[75] A. Koseska, E. Volkov, J. Kurths, Synthetic multicellular oscillatory systems: controlling protein dynamics with genetic circuits, Phys. Scr. 84 (2011) 045007.
[76] A. Koseska, A. Zaikin, J. Kurths, J. Garcia-Ojalvo, Timing cellular decision making under noise via cell–cell communication, PLoS One 4 (2009) e4872.
[77] T.S. Gardner, C.R. Cantor, J.J. Collins, Construction of a genetic toggle switch in escherichia coli, Nature 403 (2000) 339–342.
[78] J. Foss, A. Longtin, B. Mensour, J. Milton, Multistability and delayed recurrent loops, Phys. Rev. Lett. 76 (1996) 708–711.
[79] A. Takamatsu, R. Tanaka, H. Yamada, T. Nakagaki, T. Fujii, I. Endo, Spatiotemporal symmetry in rings of coupled biological oscillators of physarum plasmodial slime mold, Phys. Rev. Lett. 87 (2001) 078102.
[80] S. Yanchuk, M. Wolfrum, Destabilization patterns in chains of coupled oscillators, Phys. Rev. E 77 (2008) 026212.
[81] P. Perlikowski, S. Yanchuk, O.V. Popovych, P.A. Tass, Periodic patterns in a ring of delay-coupled oscillators, Phys. Rev. E 82 (2010) 036208.
[82] A. Koseska, J. Kurths, Topological structures enhance the presence of dynamical regimes in synthetic networks, Chaos 20 (2010) 045111.
[83] D.S. Chernavskii, E.K. Palamarchuk, A.A. Polezhaev, G.I. Solyanik, E.B. Burakova, A mathematical model of periodic processes in membranes (with application to cell cycle regulation), BioSystems 9 (1977) 187–193.
[84] J. Henquin, J.C. Jonas, P. Gilon, Functional significance of Ca^{2+} oscillations in pancreatic β-cells, Diabetes Metab. 47 (1998) 1266–1273.
[85] M. Zarkovic, J.C. Henquin, Synchronization and entrainment of cytoplasmic Ca^{2+} oscillations in cell clusters prepared from single or multiple mouse pancreatic islets, Am. J. Physiol. Endocrinol. Metab. 287 (2004) E340–E347.
[86] E. Ullner, A. Koseska, J. Kurths, E. Volkov, H. Kantz, J. García-Ojalvo, Multistability of synthetic genetic networks with repressive cell-to-cell communication, Phys. Rev. E 78 (2008) 031904.
[87] M. Yoshimoto, K. Yoshikawa, Y. Mori, Coupling among three chemical oscillators: synchronization, phase death, and frustration, Phys. Rev. E 47 (1993) 864–874.
[88] K. Bar-Eli, Coupling of identical chemical oscillators, J. Phys. Chem. 94 (1990) 2368–2374.
[89] J. Tyson, S. Kauffman, Control of mitosis by a continuous biochemical oscillation: synchronization;spatially inhomogeneous oscillations, J. Math. Biol. 1 (1975) 289–310.
[90] H.C. Berg, Coli in Motion, Springer, New York, 2004.
[91] M.G. Rosenblum, A. Pikovsky, J. Kurths, Phase synchronization in driven and coupled chaotic oscillators, IEEE Trans. Circuit. Syst. 44 (1997) 874.
[92] W. Liu, J.H. Xiao, X.L. Qian, J. Yang, Antiphase synchronization in coupled chaotic oscillators, Phys. Rev. E 73 (2006) 057203.
[93] A. Stefanoski, T. Kapitanik, Steady state locking in coupled chaotic systems, Phys. Lett. A 210 (1996) 279.
[94] G. Osipov, A. Pikovsky, M. Rosenblum, J. Kurths, Phase synchronization effects in a lattice of nonidentical Rössler oscillators, Phys. Rev. E 55 (1997) 2353–2361.
[95] J. Ryu, W. Kye, S. Lee, M. Kim, M. Choi, S. Rim, Y. Park, C. Kim, Effects of time-delayed feedback on chaotic oscillators, Phys. Rev. E 70 (2004) 036220.
[96] Y. Chen, J. Xiao, W. Liu, L. Li, Y. Yang, Dynamics of chaotic systems with attractive and repulsive couplings, Phys. Rev. E 80 (2009) 046206.
[97] A.S. Pikovsky, M.I. Rabinovich, A simple self-sustained generator with stochastic behavior, Sov. Phys. Dokl. 23 (1978) 183.
[98] S. Grossberg, Pattern formation by the global limits of a nonlinear competitive interaction in n dimensions, J. Math. Biol. 4 (1977) 237–256.
[99] K. Gurney, T.J. Prescott, P. Redgrave, A computational model action selection in the basal ganglia (i): a new functional anatomy, Biol. Cybernet. 84 (2001) 401–410.
[100] Z.H. Mao, S.G. Massaquoi, Dynamics of winner-take-all competition in recurrent neural networks with lateral inhibition, IEEE Trans. Neural Netw. 18 (2007) 55–69.
[101] S. Moldakarimov, J.E. Rollenhagen, C.R. Olson, C.C. Chow, Competitive dynamics in cortical responses to visual stimuli, J. Neurophysiol. 94 (2005) 3388–3396.
[102] L. Rubchinsky, M. Sushchik, Disorder can eliminate oscillator death, Phys. Rev. E 62 (2000) 6440–6446.
[103] M.N. Stolyarov, V.A. Romanov, E. Volkov, Out-of-phase mixed-mode oscillations of two strongly coupled identical relaxation oscillators, Phys. Rev. E 54 (1996) 163–169.
[104] J. Hudson, M. Hart, D. Marinko, An experimental study of multiple peak periodic and nonperiodic oscillations in the Belousov-Zhabotinskii reaction, J. Chem. Phys. 71 (1979) 1601–1606.
[105] V. Petrov, S.K. Scott, K. Showalter, Mixed-mode oscillations in chemical systems, J. Chem. Phys. 97 (1992) 6191–6198.
[106] A. Kuznetsov, N. Kopell, C. Wilson, Transient high-frequency firing in a coupled-oscillator model of the mesencephalic dopaminergic neuron, J. Neurophysiol. 95 (2006) 932–947.
[107] M. Mikikian, M. Cavarroc, L. Couedel, Y. Tessier, L. Boufendi, Mixed-mode oscillations in complex-plasma instabilities, Phys. Rev. Lett. 100 (2008) 225005.
[108] C.A. del Negro, C.G. Wilson, R.J. Butera, H. Rigatto, J.C. Smith, Periodicity, mixed-mode oscillations, and quasiperiodicity in a rhythm-generating neural network, Biophys. J. 82 (2002) 206–214.
[109] A.A. Alonso, R.R. Linas, Subthreshold Na^{+}-dependent theta like rhythmicity in stellate cells of entorhinal cortex layer II, Nature 342 (1989) 175–177.
[110] Y. Yamaguchi, H. Shimizu, Theory of self-synchronization in the presence of native frequency distribution and external noises, Physica D 11 (1984) 212–226.
[111] D.G. Aronson, G.B. Ermentrout, N. Koppel, Amplitude response of coupled oscillators, Physica D 41 (1990) 403.
[112] Z. Neufeld, I. Kiss, C. Zhou, J. Kurths, Synchronization and oscillator death in oscillatory media with stirring, Phys. Rev. Lett. 91 (2003) 084101.
[113] V. Astakhov, S. Koblyanski, A. Shabunin, T. Kapitaniak, Peculiarities of the transitions to synchronization in coupled systems with amplitude death, Chaos 21 (2011) 023127.
[114] Y. Zhai, I.Z. Kiss, J.L. Hudson, Amplitude death through a Hopf bifurcation in coupled electrochemical oscillators: experiments and simulations, Phys. Rev. E 69 (2004) 026208.
[115] M. Wei, J. Lun, Amplitude death in coupled chaotic solid-state lasers with cavity-configuration-dependent instabilities, Appl. Phys. Lett. 91 (2007) 061121.
[116] A.K. Kryukov, V.S. Petrov, L.S. Averyanova, G.V. Osipov, W. Chen, O. Drugova, C.K. Chan, Synchronization phenomena in mixed media of passive, excitable, and oscillatory cells, Chaos 18 (2008) 037129.
[117] D.V.R. Reddy, A. Sen, G.L. Johnston, Time delay induced death in coupled limity cycle oscillators, Phys. Rev. Lett. 80 (1998) 5109–5112.
[118] D.V.R. Reddy, A. Sen, G.L. Johnston, Time delay effects on coupled limit cycle oscillators at Hopf bifurcation, Physica D 129 (1999) 15–34.
[119] F.M. Atay, Distributed delays facilitate amplitude death of coupled oscillators, Phys. Rev. Lett. 91 (2003) 094101.

[120] R. Dodla, A. Sen, G.L. Johnston, Phase-locked patterns and amplitude death in a ring of delay-coupled limit cycle oscillators, Phys. Rev. E 69 (2004) 056217.
[121] R. Herrero, M. Figueras, J. Rius, F. Pi, G. Orriols, Experimental oscillations of the amplitude death effect in two coupled nonlinear oscillators, Phys. Rev. Lett. 84 (2000) 5312–5315.
[122] D.V.R. Reddy, A. Sen, G.L. Johnston, Experimental evidence of time-delay-induced death in coupled limity cycle oscillators, Phys. Rev. Lett. 85 (2000) 3381–3384.
[123] R. Karnatak, R. Ramaswamy, A. Prasad, Amplitude death in the absence of time delays in identical coupled oscillators, Phys. Rev. E 76 (2007) 035201(R).
[124] W. Zou, C. Yao, M. Zhan, Eliminating delay-induced oscillation death by gradient coupling, Phys. Rev. E 82 (2010) 056203.
[125] J. Yang, Transition to amplitude death in a regular array of nonlinear oscillators, Phys. Rev. E 76 (2007) 016204.
[126] V. Resmi, G. Ambika, R. Amritkar, General mechanism for amplitude death in coupled systems, Phys. Rev. E 84 (2011) 046212.
[127] L. Rubchinsky, M. Sushchik, G. Osipov, Patterns in networks of oscillators formed via synchronization and oscillator death, Math. Comput. Simul. 58 (2002) 443–467.
[128] W. Liu, J. Xiao, J. Yang, Partial amplitude death in coupled chaotic oscillators, Phys. Rev. E 72 (2005) 057201.
[129] E. Volkov, M. Stolyarov, Temporal variability generated by coupling of mitotic timers, J. Biol. Syst. 3 (1995) 63–78.
[130] S. Smale, A mathematical model of two cells via Turing's equation, in: J.R Marsden, M. McCracken (Eds.), The Hopf Bifurcation and its Application, Springer-Verlag, New York, Heidelberg, Berlin, 1974.
[131] C. Morris, H. Lecar, Voltage oscillations in the barnacle giant muscle fiber, Biophys. J. 35 (1981) 193–213.